†Electronic supplementary information (ESI)

Development of ruthenium complexes with S-donor ligands for application in synthesis and, catalytic acceptorless alcohol dehydrogenation and crossed-aldol condensation†

Anushri Chandra,[a] Pousali Basu,[a] Shreya Raha,[a,§] Papu Dhibar[a,b] and Samaresh Bhattacharya*[a]

[a] *Department of Chemistry, Inorganic Chemistry Section, Jadavpur University, Kolkata - 700 032, India. E-mail: samareshb.chemistry@jadavpuruniversity.in*

[b] *Department of Chemistry, Brainware University, Kolkata 700 125, India*

Contents:

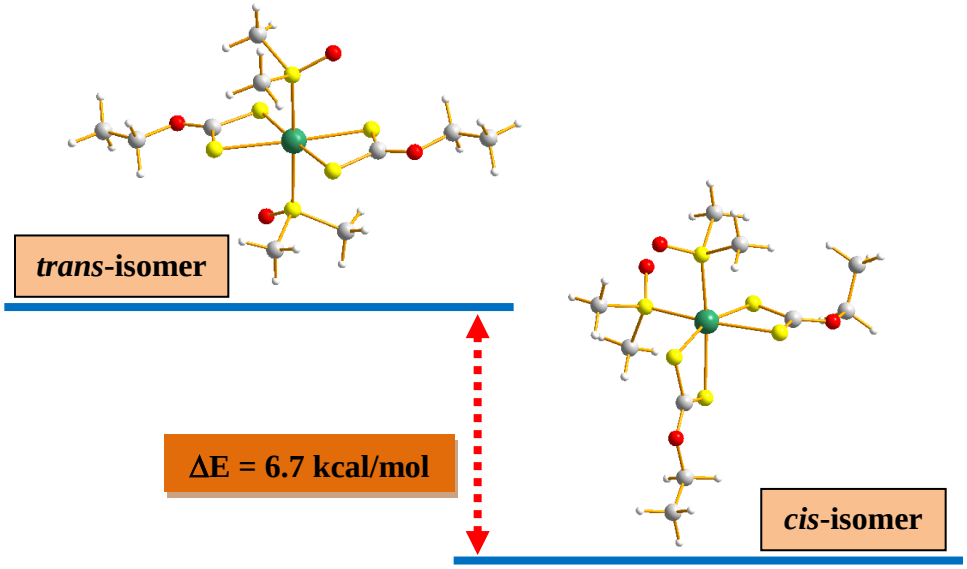

Fig. S1 DFT-optimized structures of the *trans* and *cis* isomers of $[Ru(L^2)_2(dmso)_2]$, and the energy difference (ΔE) between them.

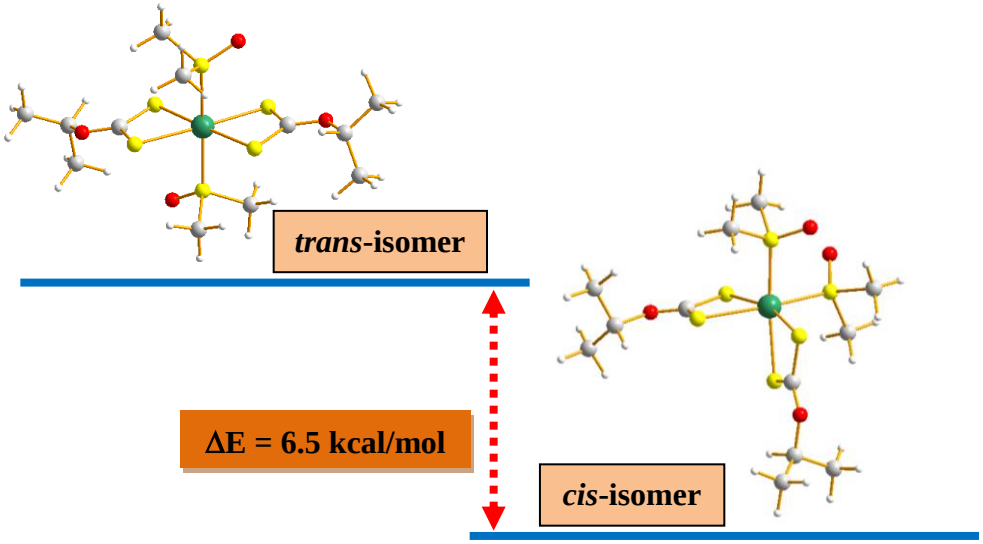

Fig. S2 DFT-optimized structures of the *trans* and *cis* isomers of $[Ru(L^3)_2(dmso)_2]$, and the energy difference (ΔE) between them.

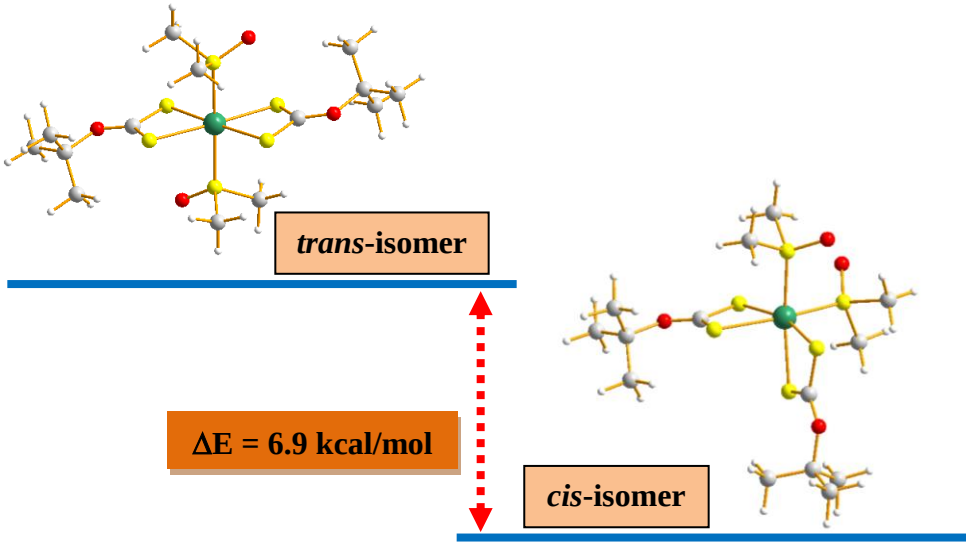

Fig. S3 DFT-optimized structures of the *trans* and *cis* isomers of $[Ru(L^4)_2(dmso)_2]$, and the energy difference (ΔE) between them.

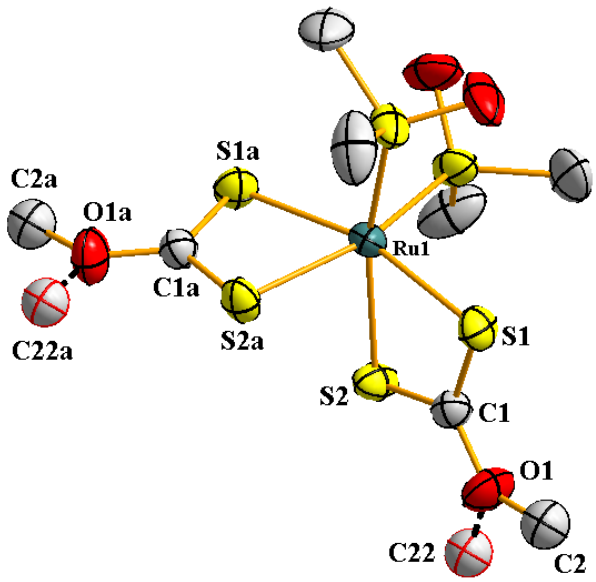

Fig. S4 Molecular structure of $[Ru(L^1)_2(dmso)_2]$ showing the disordered methyl carbons (C2, C22 and C2a, C22a).

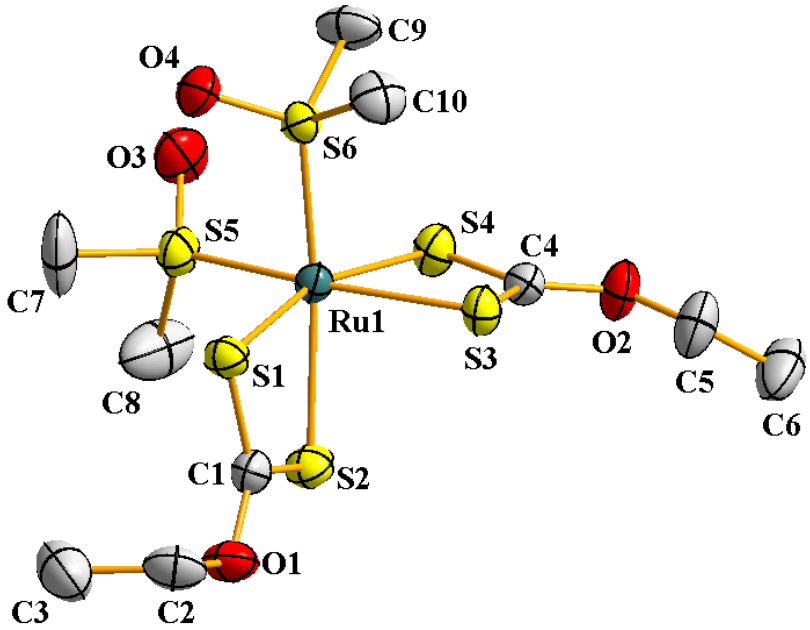

Fig. S5 Molecular structure of $[Ru(L^2)_2(dmso)_2]$.

Table S1 Selected bond distances and bond angles for $[Ru(L^2)_2(dmso)_2]$

Bond distances (Å)			
Ru1-S1	2.3904(9)	C4-S3	1.684(4)
Ru1-S2	2.4441(11)	C4-S4	1.690(3)
Ru1-S3	2.4337(11)	S5-O3	1.473(3)
Ru1-S4	2.3977(10)	S6-O4	1.478(3)
Ru1-S5	2.2602(11)	C1-O1	1.320(4)
Ru1-S6	2.2592(10)	C2-O1	1.457(4)
C1-S1	1.696(4)	C4-O2	1.329(4)
C1-S2	1.688(4)	C5-O2	1.455(5)
Bond angles (°)			
S1-Ru1-S4	162.82(4)	S1-Ru1-S2	72.15(3)
S2-Ru1-S6	166.61(3)	S3-Ru1-S4	72.29(3)
S3-Ru1-S5	166.72(4)		

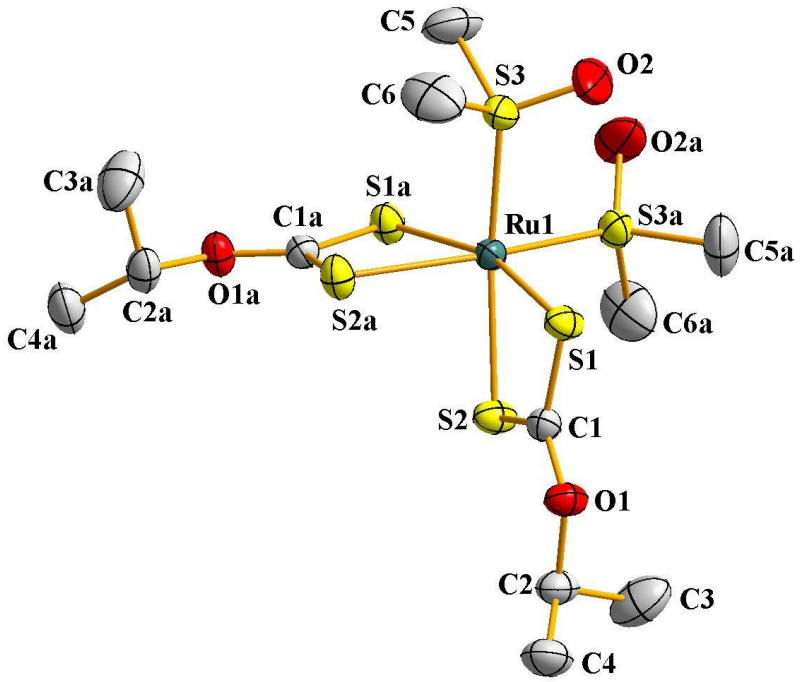

Fig. S6 Molecular structure of $[Ru(L^3)_2(dmso)_2]$.

Table S2 Selected bond distances and bond angles for $[Ru(L^3)_2(dmso)_2]$

Bond distances (Å)			
Ru1-S1	2.4028(5)	C1-S1	1.6946(19)
Ru1-S2	2.4232(6)	C1-S2	1.698(2
Ru1-S3	2.2577(6)	C1-O1	1.315(2)
S3-O2	1.474(2)	C2-O1	1.473(3)
Bond angles (°)			
S1-Ru1-S1a	162.96(2)	S2a-Ru1-S3a	166.08(2)
S2-Ru1-S3	166.08(2)	S1-Ru1-S2	72.34(2)

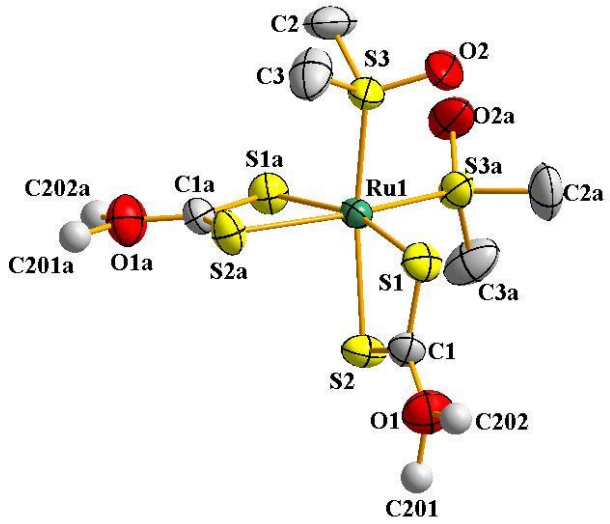

Fig. S7 Molecular structure of $[Ru(L^4)_2(dmso)_2]$ showing the disordered central carbons of the *tert*-butyl groups (C201, C202 and C201a, C202a). The other three carbons of the *tert*-butyl groups are not shown, as they suffer from heavy disorder problem.

Table S3 Selected bond distances and bond angles for $[Ru(L^4)_2(dmso)_2]$

Bond distances (Å)			
Ru1-S1	2.3865(11)	C1-S1	1.682(4)
Ru1-S2	2.4449(13)	C1-S2	1.685(5)
Ru1-S3	2.2532(13)	C1-O1	1.343(6)
S3-O2	1.476(4)		
Bond angles (°)			
S1-Ru1-S1a	164.15(38)	S1-Ru1-S2	71.99(40)
S2-Ru1-S3	164.22(43)		

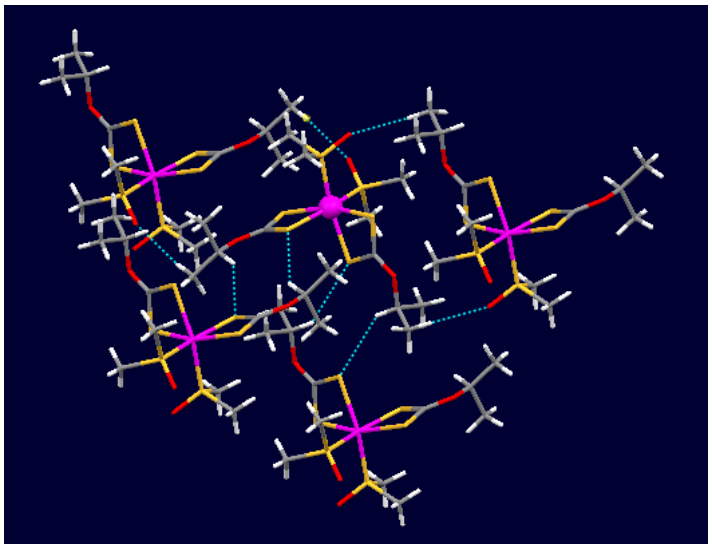

Fig. S8 Intermolecular C-H···S and C-H···O interactions in the lattice of $[Ru(L^3)_2(dmso)_2]$.

Table S4 Selected bond distances and bond angles for $[Ru(L^3)_2(bpy)]$

Bond distances (Å)			
Ru1-S1	2.3935(9)	C5-O2	1.315(5)
Ru1-S2	2.3904(7)	C1-S1	1.693(3)
Ru1-S3	2.395(1)	C1-S2	1.683(4)
Ru1-S4	2.3912(7)	C1-O1	1.328(5)
Ru1-N1	2.055(2)	C2-O1	1.476(5)
Ru1-N2	2.061(2)	C2-C3	1.502(7)
C5-S3	1.695(3)	C2-C4	1.490(6)
C5-S4	1.683(4)		
Bond angles (°)			
S1-Ru1-S3	163.79(3)	S1-Ru1-S2	72.60(3)
S2-Ru1-N1	174.08(7)	S3-Ru1-S4	72.60(3)
S4-Ru1-N2	171.97(3)	N1-Ru1-N2	78.28(8)

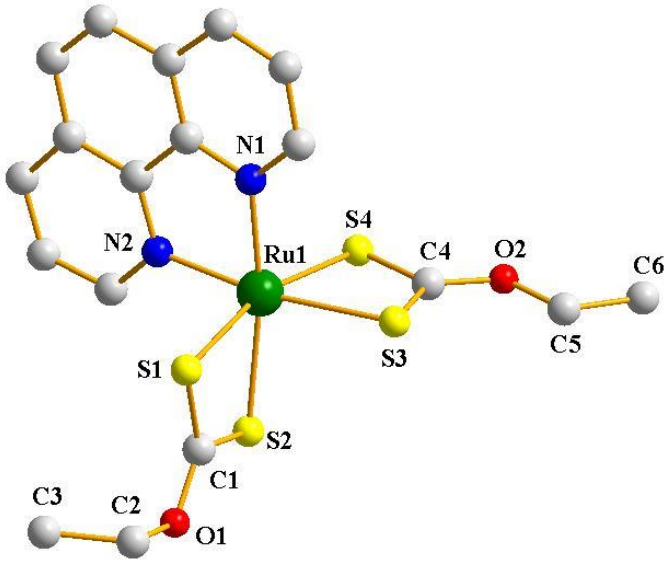

Fig. S9 DFT-optimized structure of $[Ru(L^2)_2(phen)]$.

Table S5 Some computed bond distances and bond angles for $[Ru(L^2)_2(phen)]$

Bond distances (Å)			
Ru1-S1	2.4812	C1-S1	1.7164
Ru1-S2	2.4810	C1-S2	1.7052
Ru1-S3	2.4846	C1-O1	1.3305
Ru1-S4	2.4702	C2-O1	1.4486
Ru1-N1	2.0970	C4-S3	1.7106
Ru1-N2	2.0929	C4-S4	1.7084
		C4-O2	1.3295
		C5-O2	1.4465
Bond angles (°)			
S1-Ru1-S4	163.523	S1-Ru1-S2	71.737
S2-Ru1-N1	169.983	S3-Ru1-S4	71.879
S3-Ru1-N2	169.517	N1-Ru1-N2	78.965

Table S6 Computed parameters from TDDFT calculations on $[Ru(L^1)_2(dmso)_2]$ for electronic spectral properties in dichloromethane solution

Excited State	Composition	CI value	*E* (eV)	Oscillator strength (*f*)	λ_{theo} (nm)	Assignment	λ_{exp} (nm)
9	H-1 → L	0.54398	3.7074	0.0151	334.43	MLCT/LLCT	346
	H-1 → L+1	0.28212				MLCT/LLCT	
	H → L	0.15373				MLCT/LLCT	
	H→ L+1	0.26411				MLCT/LLCT	
26	H-7 → L+2	0.20556	5.0205	0.1389	246.95	LMCT/ LLCT	284
	H-7 → L+3	0.17035				LMCT/LLCT	
	H-6 → L+2	0.50223				LMCT/LLCT	
	H-5 → L+2	0.29678				LMCT	
	H-3 → L+3	0.14770				LMCT	
	H → L+2	0.11650				LLCT /LMCT	
74	H-13 → L+3	0.20601	6.3603	0.0985	194.94	LMCT/LLCT	236
	H-3 → L+4	0.21991				LMCT	
	H-2 → L+7	0.13528				LMCT	
	H-1 → L+8	0.10349				MLCT/LLCT	
	H-1 → L+9	0.15416				MLCT/LLCT	
	H-1 → L+12	0.10071				MLCT/LLCT	
	H→ L+11	0.50848				MLCT/LLCT	

Table S7 Compositions of selected molecular orbitals of $[Ru(L^1)_2(dmso)_2]$ associated with the electronic spectral transitions

% Contribution of fragments to	Fragments				
	Ru	L^1 (1)	L^1 (2)	DMSO (1)	DMSO (2)
HOMO (H)	50	8	38	1	3
H-1	50	38	7	3	2
H-2	66	17	12	3	2
H-3	7	36	34	10	13
H-5	7	15	17	31	30
H-6	27	14	31	8	20
H-7	30	26	18	21	5
H-13	21	37	38	2	2
LUMO (L)	6	58	35	0	1
L+1	4	35	60	0	1
L+2	53	11	16	13	7
L+3	52	24	17	1	6
L+4	87	0	0	6	7
L+7	91	3	3	3	0
L+8	11	30	6	32	21
L+9	23	1	18	21	37
L+11	13	42	4	39	2
L+12	9	11	19	31	30

HOMO (H) 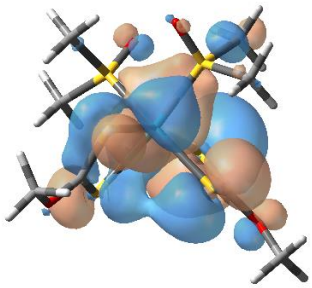	H-1 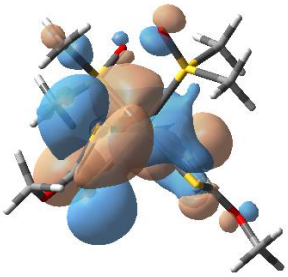	H-2 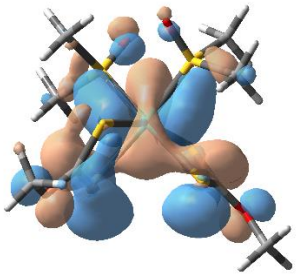	H-3 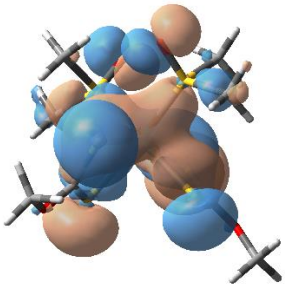
H-5 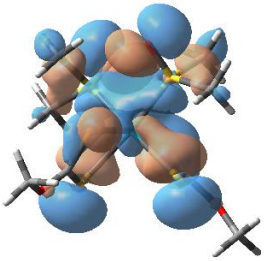	H-6 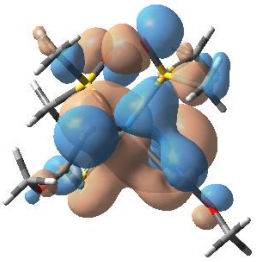	H-7 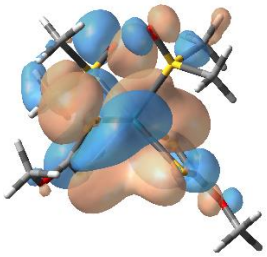	H-13 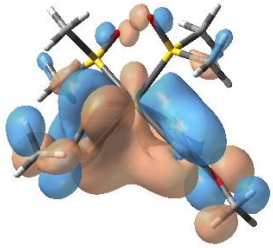
LUMO (L) 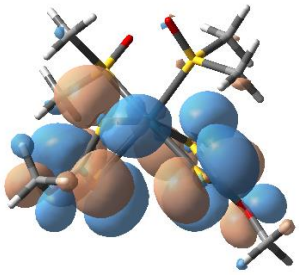	L+1 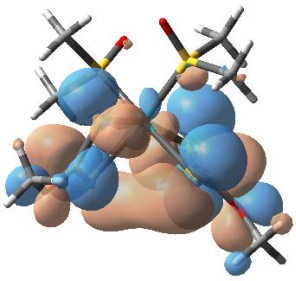	L+2 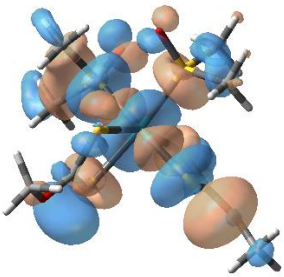	L+3 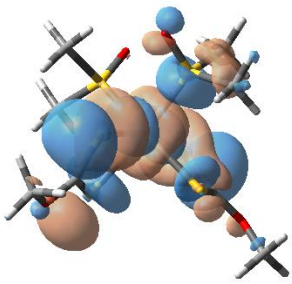
L+4 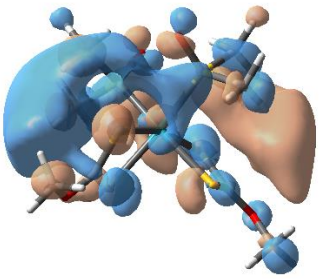	L+7 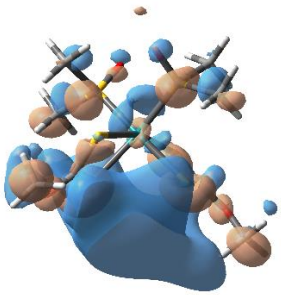	L+8 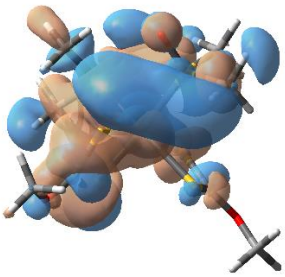	L+9 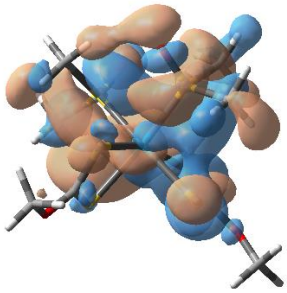

L+11	L+12		
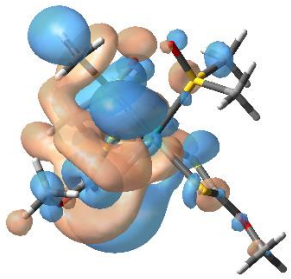	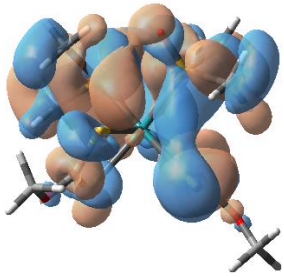		

Fig. S10 Contour plots of the molecular orbitals of $[Ru(L^1)_2(dmso)_2]$, which are associated with the electronic spectral transitions (See **Table S6**).

Table S8 Computed parameters from TDDFT calculations on $[Ru(L^2)_2(dmso)_2]$ for electronic spectral properties in dichloromethane solution

Excited State	Composition	CI value	*E* (eV)	Oscillator strength (*f*)	λ_{theo} (nm)	Assignment	λ_{exp} (nm)
9	H-1 → L	0.60432	3.7162	0.0160	333.64	MLCT/LLCT	347
	H-1 → L+1	0.14342				MLCT/LLCT	
	H→ L+1	0.27974				MLCT/LLCT	
26	H-7 → L+2	0.25423	5.0233	0.1430	246.82	LMCT/ LLCT	285
	H-7 → L+3	0.13889				LMCT/LLCT	
	H-6 → L+2	0.48971				LMCT/LLCT	
	H-3 → L+3	0.14097				LMCT	
	H → L+2	0.12147				LLCT/LMCT	
72	H-13 → L+1	0.11096	6.3243	0.1163	196.04	MLCT/LLCT	237
	H-13 → L+3	0.21573				LMCT/LLCT	
	H-12 → L+2	0.17009				LMCT/LLCT	
	H-4 → L+4	0.20482				LMCT/LLCT	
	H-3 → L+4	0.30120				LMCT	
	H-2 → L+7	0.17294				LMCT	
	H-2 → L+8	0.22678				MLCT/LLCT	
	H-1 → L+9	0.26937				MLCT/LLCT	
	H-1 → L+10	0.18582				MLCT/LLCT	

Table S9 Compositions of selected molecular orbitals of $[Ru(L^2)_2(dmso)_2]$ associated with the electronic spectral transitions

% Contribution of fragments to	Fragments				
	Ru	L^2 (1)	L^2 (2)	DMSO (1)	DMSO (2)
HOMO (H)	50	9	37	1	3
H-1	50	37	9	2	2
H-2	65	18	12	3	2
H-3	9	37	34	8	12
H-4	17	36	37	5	5
H-6	26	14	30	9	21
H-7	31	27	18	20	4
H-12	28	24	29	11	8
H-13	21	34	41	2	2
LUMO (L)	6	62	31	0	1
L+1	4	32	64	0	0
L+2	53	10	16	14	7
L+3	52	24	17	1	6
L+4	86	1	0	6	7
L+7	92	0	6	2	0
L+8	11	25	5	36	23
L+9	24	1	15	23	37
L+10	11	12	36	8	33

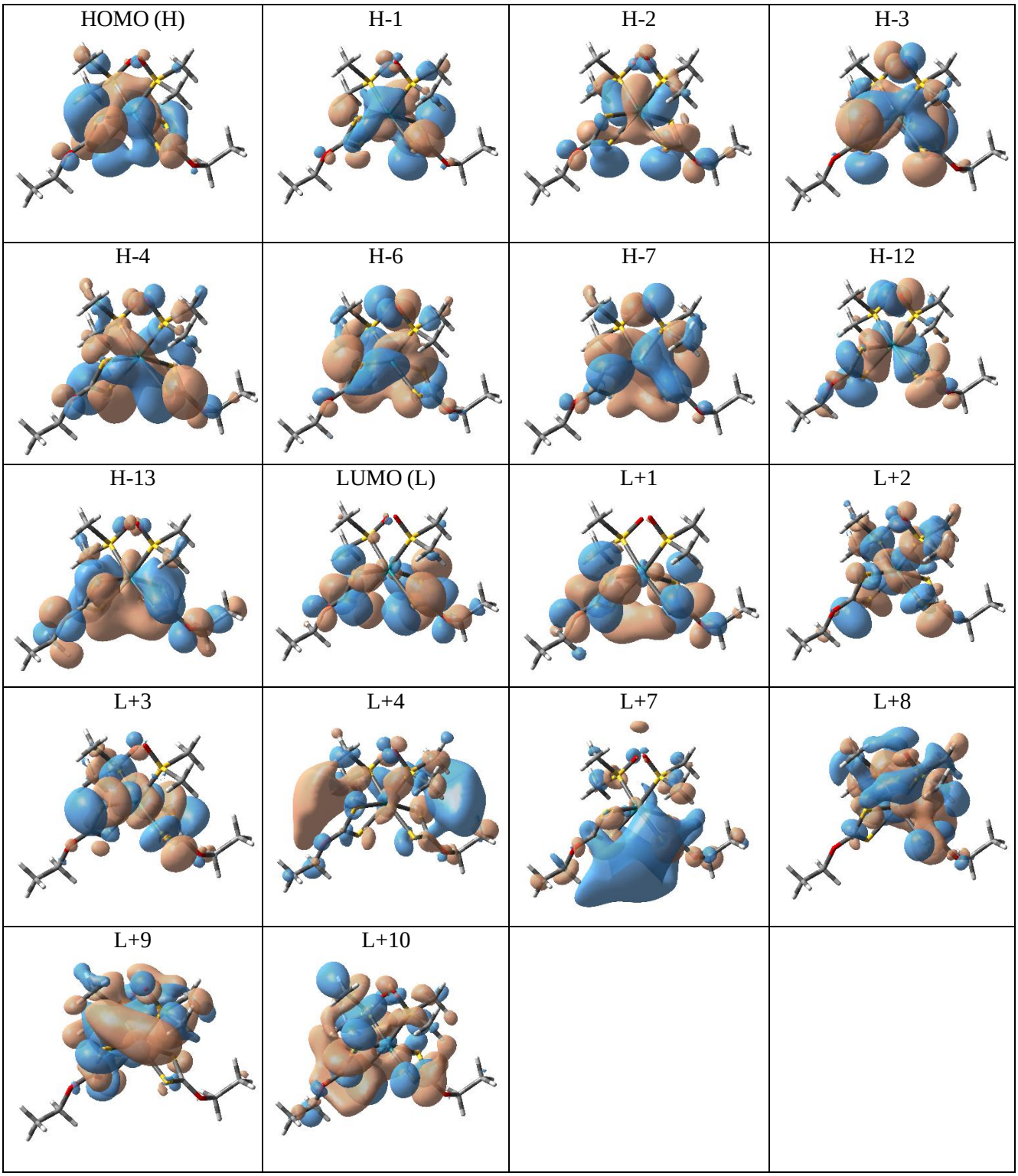

Fig. 11 Contour plots of the molecular orbitals of $[Ru(L^2)_2(dmso)_2]$, which are associated with the electronic spectral transitions (See **Table S8**).

Table S10 Computed parameters from TDDFT calculations on $[Ru(L^3)_2(dmso)_2]$ for electronic spectral properties in dichloromethane solution

Excited State	Composition	CI value	*E* (eV)	Oscillator strength (*f*)	λ_{theo} (nm)	Assignment	λ_{exp} (nm)
10	H-2 → L	0.10111	3.7320	0.0198	332.22	MLCT/LLCT	345
	H-1 → L+1	0.64772				MLCT/LLCT	
	H-1 → L+3	0.15926				MLCT/LLCT	
	H→ L	0.16827				MLCT/LLCT	
25	H-7 → L+3	0.10910	5.0142	0.1837	247.27	LMCT	286
	H-6 → L+2	0.53426				LMCT	
	H-5 → L+2	0.35139				LMCT	
	H-3 → L+3	0.14814				LMCT	
	H → L+2	0.12279				LLCT	
73	H-13 → L+3	0.16218	6.3218	0.1614	196.12	LMCT/LLCT	238
	H-12 → L+2	0.14175				LMCT/LLCT	
	H-5 → L+5	0.13576				LMCT	
	H-3 → L+4	0.25160				LMCT	
	H-2 → L+7	0.10755				LMCT/LLCT	
	H-2 → L+8	0.38866				MLCT/LLCT	
	H-1 → L+9	0.27524				LLCT/MLCT	
	H-1 → L+10	0.16223				MLCT	
	H-1 → L+12	0.15338				MLCT/LLCT	

Table S11 Compositions of selected molecular orbitals of $[Ru(L^3)_2(dmso)_2]$ associated with the electronic spectral transitions

% Contribution of fragments to	Fragments				
	Ru	L^3 (1)	L^3 (2)	DMSO (1)	DMSO (2)
HOMO (H)	50	23	23	2	2
H-1	50	23	23	2	2
H-2	65	15	14	3	3
H-3	7	37	37	10	9
H-5	7	17	17	30	29
H-6	19	19	18	22	22
H-7	40	24	24	6	6
H-12	26	28	28	9	9
H-13	22	37	37	2	2
LUMO (L)	9	45	45	0	1
L+1	4	48	48	0	0
L+2	50	14	14	11	11
L+3	52	21	21	3	3
L+4	85	4	5	3	3
L+5	73	0	0	13	14
L+7	82	7	7	2	2
L+8	12	12	10	33	33
L+9	30	6	6	29	29
L+10	8	32	32	14	14
L+12	14	15	15	28	28

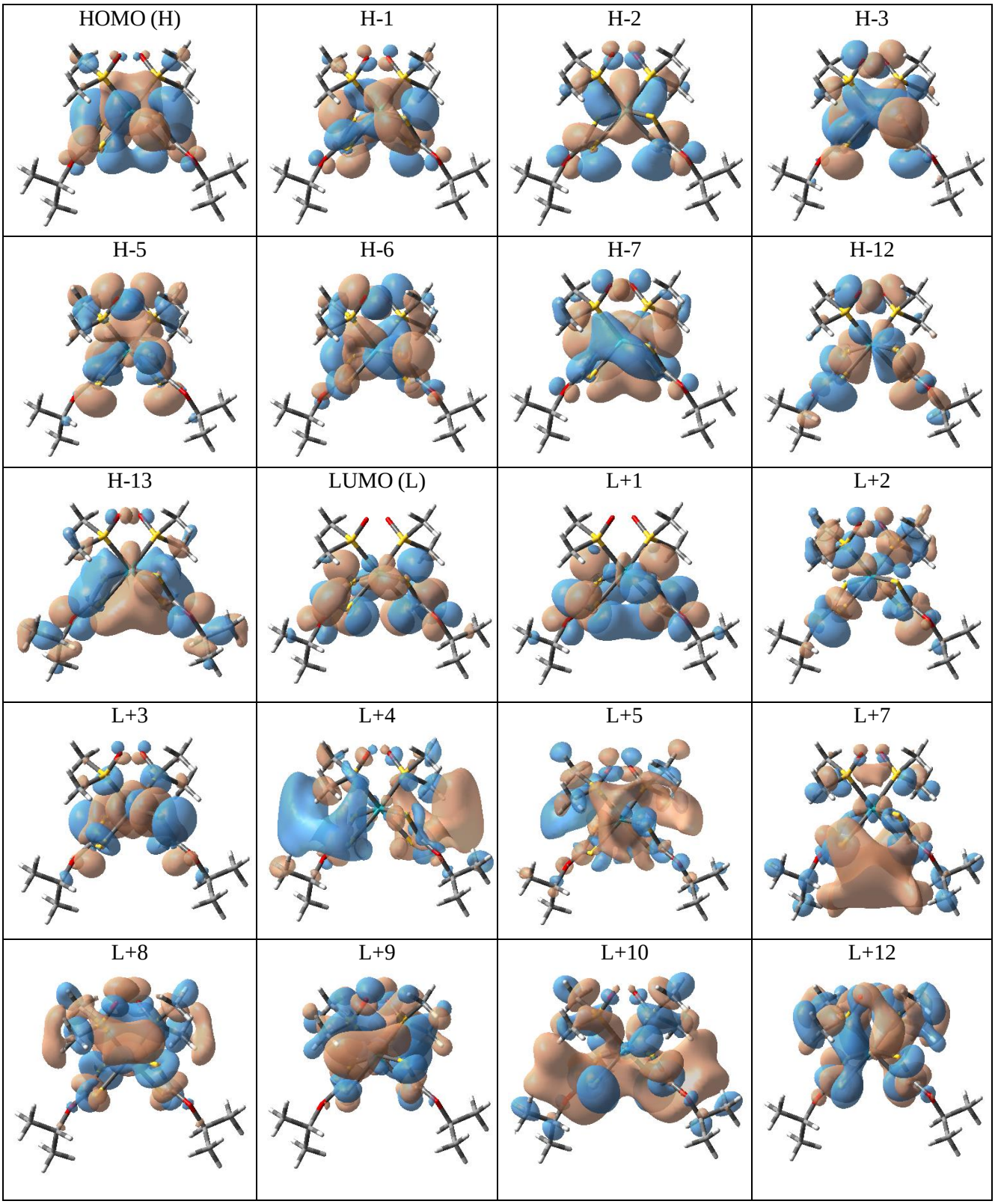

Fig. S12 Contour plots of the molecular orbitals of $[Ru(L^3)_2(dmso)_2]$, which are associated with the electronic spectral transitions (See **Table S10**).

Table S12 Computed parameters from TDDFT calculations on $[Ru(L^4)_2(dmso)_2]$ for electronic spectral properties in dichloromethane solution

Excited State	Composition	CI value	*E* (eV)	Oscillator strength (*f*)	λ_{theo} (nm)	Assignment	λ_{exp} (nm)
10	H-2 → L	0.10618	3.6858	0.0193	336.38	MLCT/LLCT	345
	H-1 → L+1	0.65694				MLCT/LLCT	
	H-1 → L+3	0.11120				MLCT/LLCT	
	H→ L	0.17414				MLCT/LLCT	
25	H-7 → L+3	0.13542	5.0234	0.1669	246.81	LMCT	283
	H-6 → L	0.16854				LLCT/MLCT	
	H-6 → L+2	0.52297				LMCT	
	H-5 → L+2	0.31405				LMCT	
	H-3 → L+3	0.16320				LMCT	
	H → L+2	0.12923				LLCT/LMCT	
74	H-16 → L+1	0.10296	6.2953	0.0945	196.95	MLCT	240
	H-15 → L	0.15666				LMCT/LLCT	
	H-14 → L+1	0.13018				MLCT/LLCT	
	H-12 → L+2	0.19600				LMCT/LLCT	
	H-4 → L+4	0.25886				LMCT	
	H-3 → L+4	0.20642				LMCT	
	H-2 → L+7	0.11601				LMCT	
	H-1 → L+9	0.28232				LLCT/MLCT	
	H-1 → L+10	0.30329				MLCT	
	H-1 → L+12	0.13713				MLCT/LLCT	
	H → L+11	0.18178				MLCT	

Table S13 Compositions of selected molecular orbitals of $[Ru(L^4)_2(dmso)_2]$ associated with the electronic spectral transitions

% Contribution of fragments to	Fragments				
	Ru	L^4 (1)	L^4 (2)	DMSO (1)	DMSO (2)
HOMO (H)	49	24	23	2	2
H-1	50	23	23	2	2
H-2	64	15	15	3	3
H-3	7	37	37	9	10
H-4	17	38	38	4	3
H-5	8	17	17	29	29
H-6	19	18	18	22	23
H-7	41	24	25	5	5
H-12	29	25	25	11	10
H-14	16	40	40	2	2
H-15	4	48	48	0	0
H-16	12	44	44	0	0
LUMO (L)	6	47	46	1	0
L+1	4	48	48	0	0
L+2	53	12	13	11	11
L+3	52	21	21	3	3
L+4	89	3	4	2	2
L+7	78	10	10	1	1
L+9	27	9	10	27	27
L+10	10	29	28	16	17
L+11	14	23	24	20	19
L+12	10	15	15	30	30

HOMO (H) 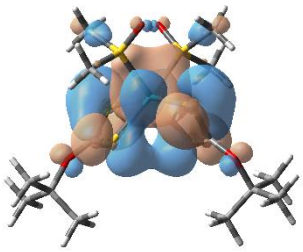	H-1 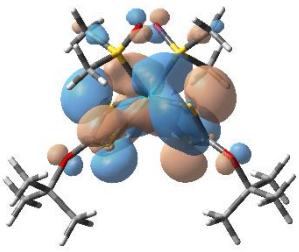	H-2 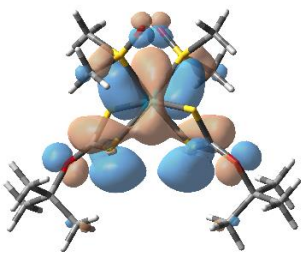	H-3 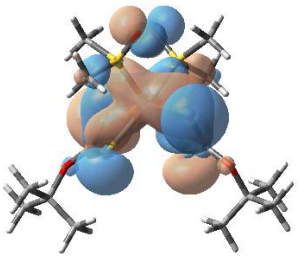
H-4 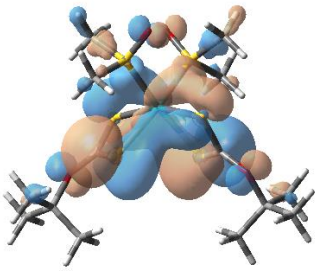	H-5 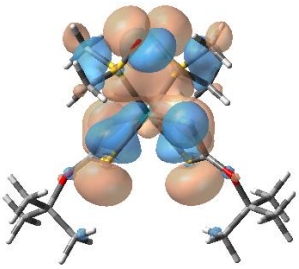	H-6 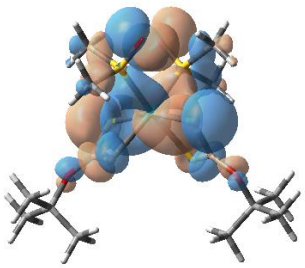	H-7 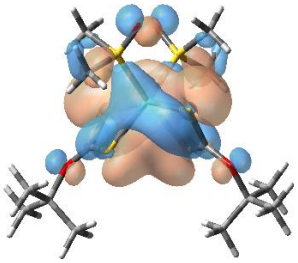
H-12 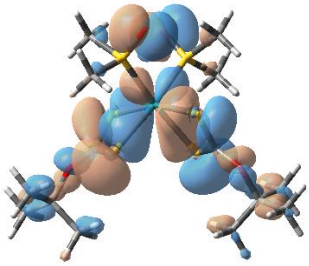	H-14 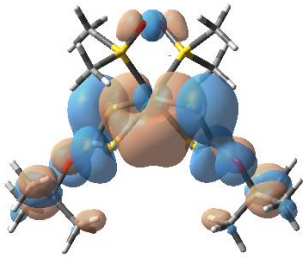	H-15 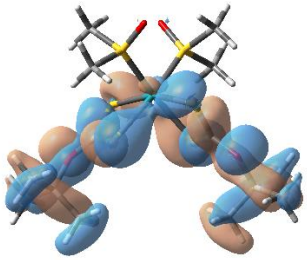	H-16 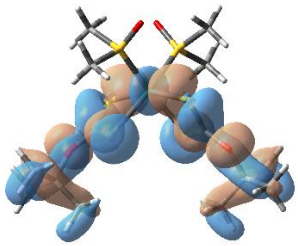
LUMO (L) 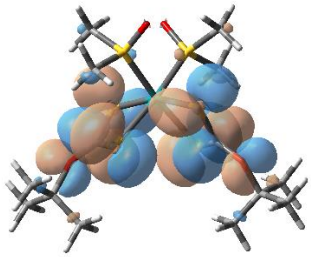	L+1 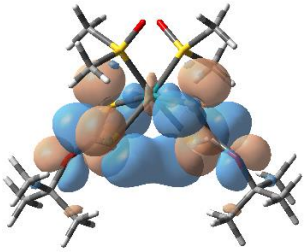	L+2 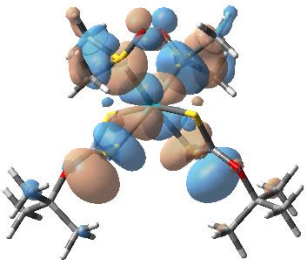	L+3 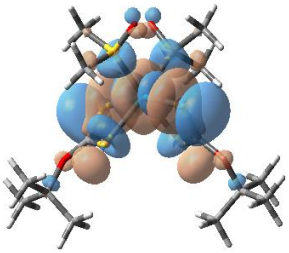

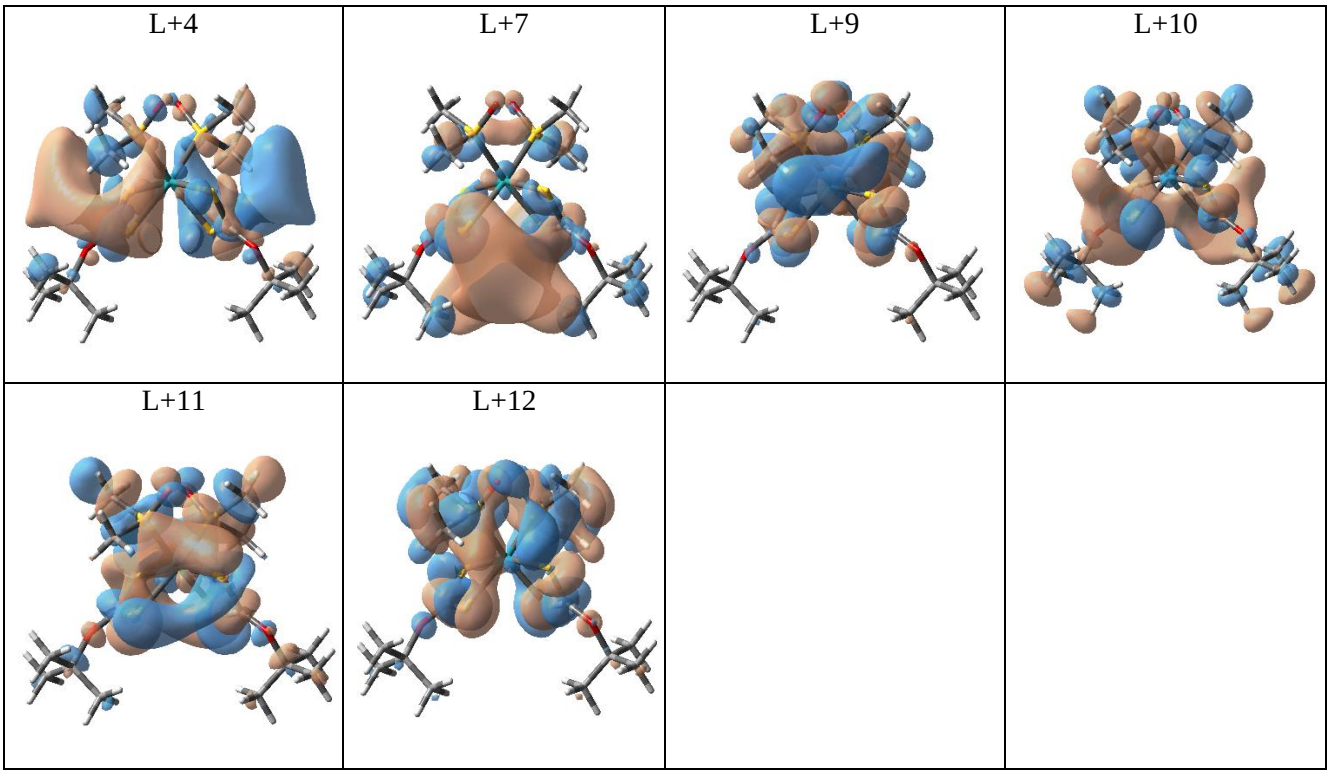

Fig. S13 Contour plots of the molecular orbitals of $[Ru(L^4)_2(dmso)_2]$, which are associated with the electronic spectral transitions (See **Table S12**).

Table S14 Computed parameters from TDDFT calculations on $[Ru(L^3)_2(bpy)]$ for electronic spectral properties in dichloromethane solution

Excited State	Composition	CI value	*E* (eV)	Oscillator strength (*f*)	λ_{theo} (nm)	Assignment	λ_{exp} (nm)
3	H-2 → L	0.38146	2.5033	0.1017	495.29	MLCT/LLCT	560
	H-1 → L	0.56561				MLCT/LLCT	
	H→ L+5	0.12297				MLCT	
14	H-2 → L+1	0.46287	3.2995	0.0384	375.77	MLCT/ LLCT	409
	H-2 → L+2	0.20042				MLCT/LLCT	
	H-1 → L+1	0.21778				MLCT/LLCT	
	H-1 → L+2	0.33870				MLCT/LLCT	
	H-1 → L+6	0.10499				LLCT/MLCT	
	H → L+4	0.19244				MLCT/LLCT	
22	H-3 → L	0.40488	3.6229	0.1456	342.22	LLCT/MLCT	378
	H-2 → L+1	0.14001				MLCT/LLCT	
	H-2 → L+4	0.41210				MLCT/LLCT	
	H-1 → L+1	0.20206				MLCT/LLCT	
	H-1 → L+3	0.10930				MLCT/LLCT	
	H-1 → L+4	0.14342				MLCT/LLCT	
	H-1 → L+6	0.10009				LLCT/MLCT	
	H→ L+4	0.16497				MLCT/LLCT	
28	H-6 → L	0.55046	4.4206	0.2723	280.47	LLCT/MLCT	299
	H-4 → L+2	0.20889				LLCT/MLCT	
	H-3 → L+2	0.25077				LLCT/MLCT	
	H-3 → L+4	0.15431				LLCT/MLCT	
48	H-5 → L+1	0.12309	5.0939	0.1981	243.40	LLCT/MLCT	290
	H-5 → L+3	0.14403				LLCT/MLCT	
	H-5 → L+4	0.13169				LLCT/MLCT	
	H-5 → L+5	0.38799				LMCT	
	H-4 → L+5	0.39837				LMCT	
	H-3 → L+5	0.15756				LMCT	
	H-3 → L+6	0.11123				LMCT/LLCT	
	H→ L+8	0.16743				LMCT	

Table S15 Compositions of selected molecular orbitals of $[Ru(L^3)_2(bpy)]$ associated with the electronic spectral transitions

% Contribution of fragments to	Fragments			
	Ru	L^3 (1)	L^3 (2)	bpy
HOMO (H)	66	14	17	3
H-1	59	15	15	11
H-2	72	12	9	7
H-3	8	44	43	5
H-4	11	45	40	4
H-5	24	32	39	5
H-6	19	38	38	5
LUMO (L)	6	1	1	92
L+1	4	1	0	95
L+2	2	0	0	98
L+3	6	92	1	1
L+4	6	1	92	1
L+5	54	20	22	4
L+6	57	14	13	16
L+8	91	4	3	2

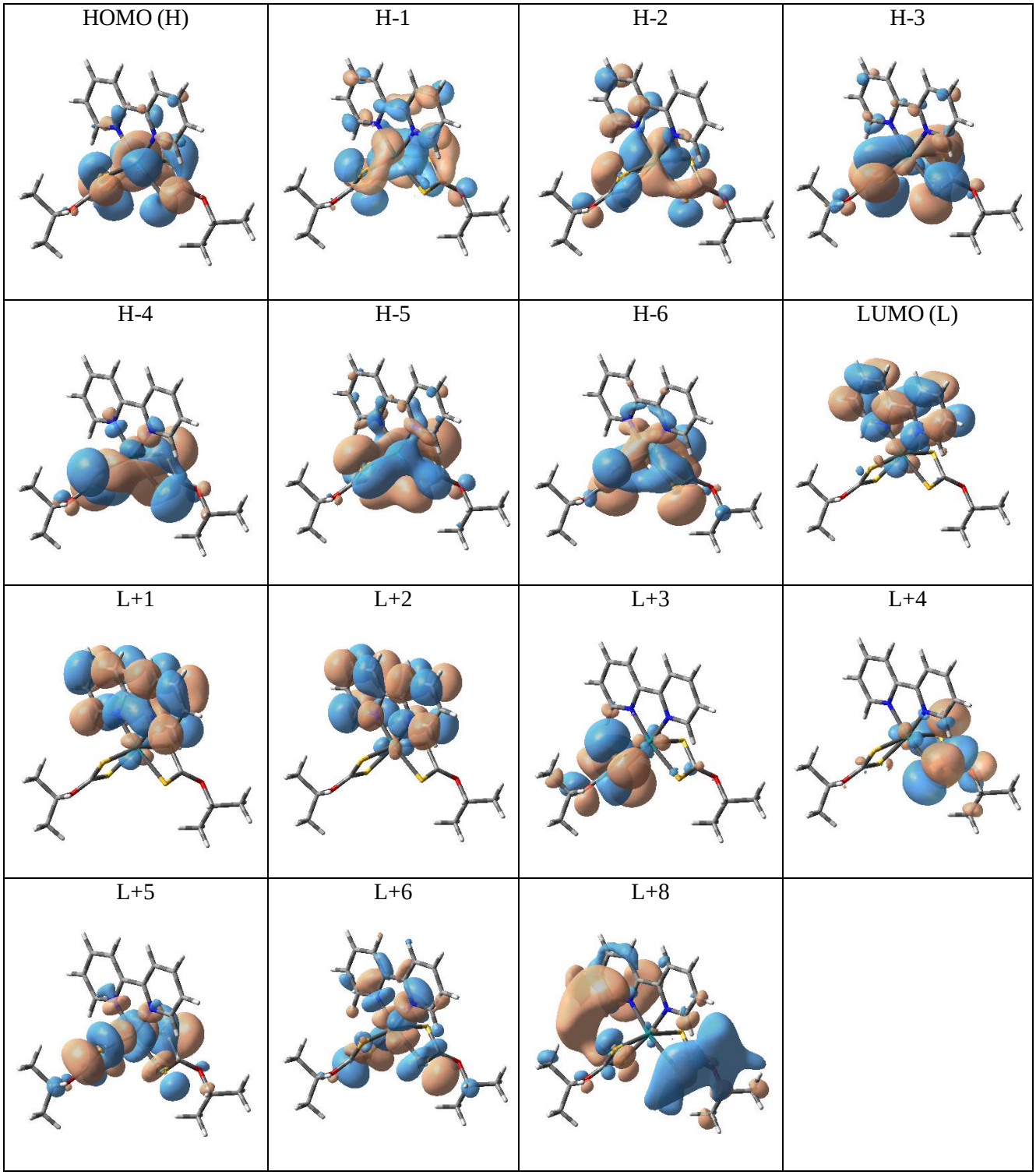

Fig. S14 Contour plots of the molecular orbitals of $[Ru(L^3)_2(bpy)]$, which are associated with the electronic spectral transitions (See **Table S14**).

Table S16 Computed parameters from TDDFT calculations on $[Ru(L^2)_2(phen)]$ for electronic spectral properties in dichloromethane solution

Excited State	Composition	CI value	*E* (eV)	Oscillator strength (*f*)	λ_{theo} (nm)	Assignment	λ_{exp} (nm)
4	H-2 → L	0.15308	2.5195	0.0443	492.11	MLCT/LLCT	540
	H-2 → L+1	0.40989				MLCT/LLCT	
	H-1 → L	0.45837				MLCT/LLCT	
	H-1→ L+1	0.14257				MLCT/LLCT	
	H→ L+1	0.22241				MLCT/LLCT	
	H→ L+5	0.14750				MLCT	
7	H-2 → L	0.10867	2.7212	0.1338	455.63	MLCT/ LLCT	496
	H-2 → L+1	0.53525				MLCT/LLCT	
	H-1 → L	0.39303				MLCT/LLCT	
	H → L+1	0.14678				MLCT/LLCT	
15	H-2 → L+2	0.19555	3.3169	0.0419	373.80	MLCT	351
	H-2 → L+3	0.52184				MLCT	
	H-1 → L+3	0.40663				MLCT	
24	H-6 → L	0.12879	3.9000	0.0440	317.91	LLCT/MLCT	324
	H-2 → L+4	0.38011				MLCT/LLCT	
	H-1 → L+4	0.54648				MLCT/LLCT	
42	H-9 → L	0.32779	4.8097	0.4374	257.78	MLCT	269
	H-8 → L	0.45029				LLCT/MLCT	
	H-8 → L+4	0.10327				LLCT/MLCT	
	H-6→ L+1	0.28400				LLCT/MLCT	
	H-5→ L+3	0.10516				MLCT/LLCT	
	H-4→ L+5	0.10628				LMCT	
	H-1→ L+7	0.12297				LLCT/LMCT	

Table S17 Compositions of selected molecular orbitals of $[Ru(L^2)_2(phen)]$ associated with the electronic spectral transitions

% Contribution of fragments to	Fragments			
	Ru	L^2 (1)	L^2 (2)	phen
HOMO (H)	66	14	17	3
H-1	57	16	15	12
H-2	74	12	8	6
H-4	12	45	39	4
H-5	24	33	38	5
H-6	19	38	37	6
H-8	23	31	33	13
H-9	1	1	1	97
LUMO (L)	7	1	1	91
L+1	1	0	0	99
L+2	6	35	11	48
L+3	5	51	31	13
L+4	4	7	52	37
L+5	54	20	22	4
L+7	58	14	13	15

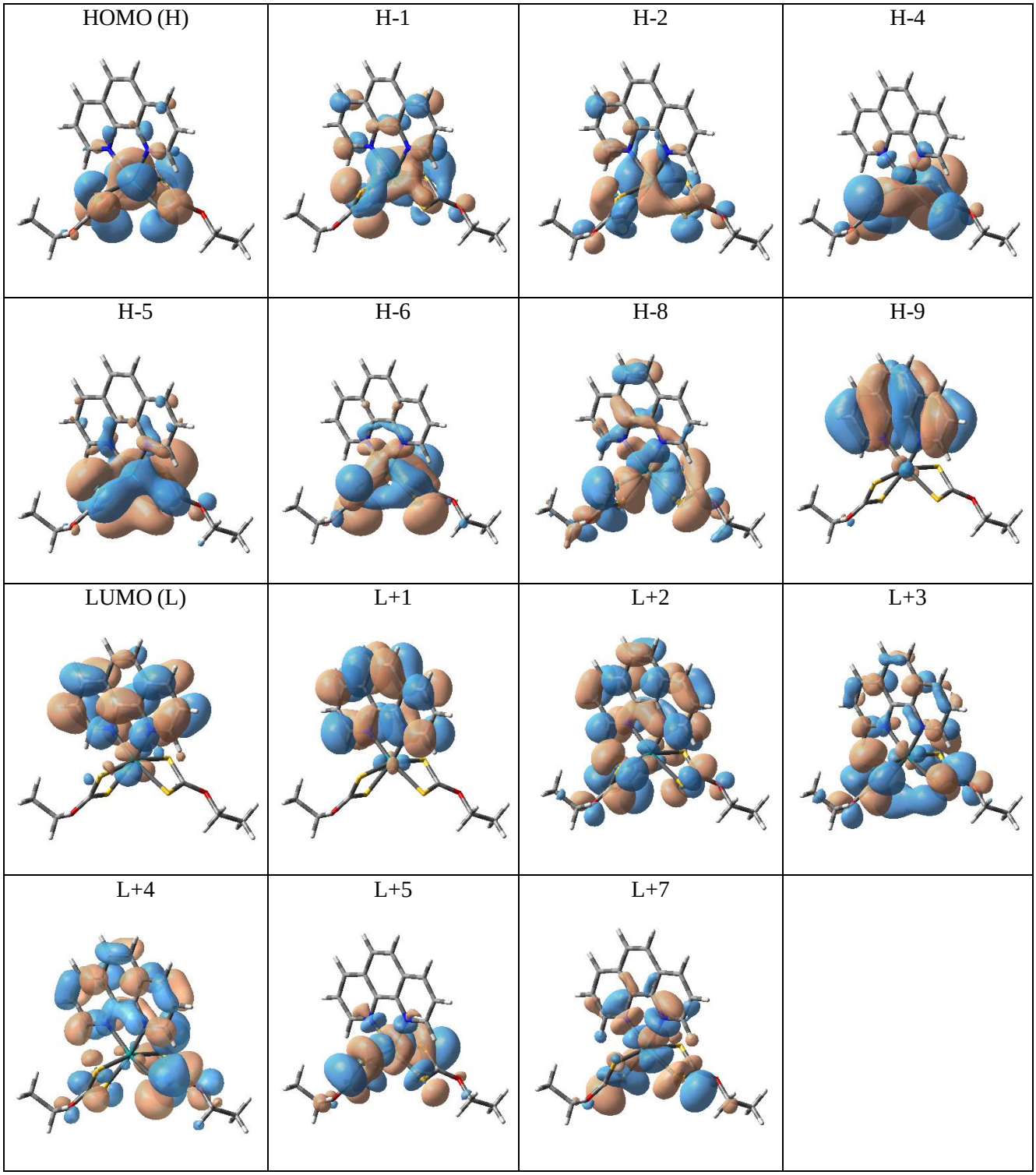

Fig. S15 Contour plots of the molecular orbitals of $[Ru(L^2)_2(phen)]$, which are associated with the electronic spectral transitions (See **Table S16**).

Table S18 Optimization of the reaction conditions for the catalysis[a]

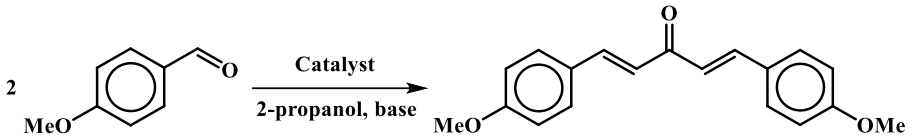

Entry	Mole % of catalyst	Solvent	Base	Mole % of base	Temp, ºC	Time, h	Yield, %
1	1	2-propanol	KOH	1	83	6	43
2	1	2-propanol	KOH	1	83	3	40
3	1	2-propanol	KOH	0.5	83	6	52
4	1	2-propanol	KO^{t}Bu	1	83	6	81
5	1	2-propanol	KO^{t}Bu	0.5	83	6	79
6	0.5	2-propanol	KO^{t}Bu	0.5	83	6	75
7	0.5	2-propanol	KO^{t}Bu	0.5	83	8	60
8	0.5	2-propanol	K_3PO_4	0.5	83	6	9
9	0.25	2-propanol	KO^{t}Bu	0.5	83	6	36
10	-	2-propanol	KO^{t}Bu	0.5	83	6	NO
11	0.5	2-propanol	-	-	83	6	NO
12	0.5	2-propanol	KO^{t}Bu	0.25	83	6	29
13	1	1-propanol	KOH	1	97	6	NO
14	1	1-propanol	KO^{t}Bu	1	97	6	NO
15	0.5	ethanol	KO^{t}Bu	0.5	78	6	NO
16[b]	0.5	2-propanol	KO^{t}Bu	0.5	83	6	73
17[c]	0.5	2-propanol	KO^{t}Bu	0.5	83	6	75
18[d]	0.5	2-propanol	KO^{t}Bu	0.5	83	6	70

[a] Reaction conditions: Catalyst, $[Ru(L^3)_2(dmso)_2]$; substrate, 4-methoxybenzaldehyde (1 mmol); solvent (5.0 mL).
[b] Catalyst, $[Ru(L^1)_2(dmso)_2]$
[c] Catalyst, $[Ru(L^2)_2(dmso)_2]$
[d] Catalyst, $[Ru(L^4)_2(dmso)_2]$

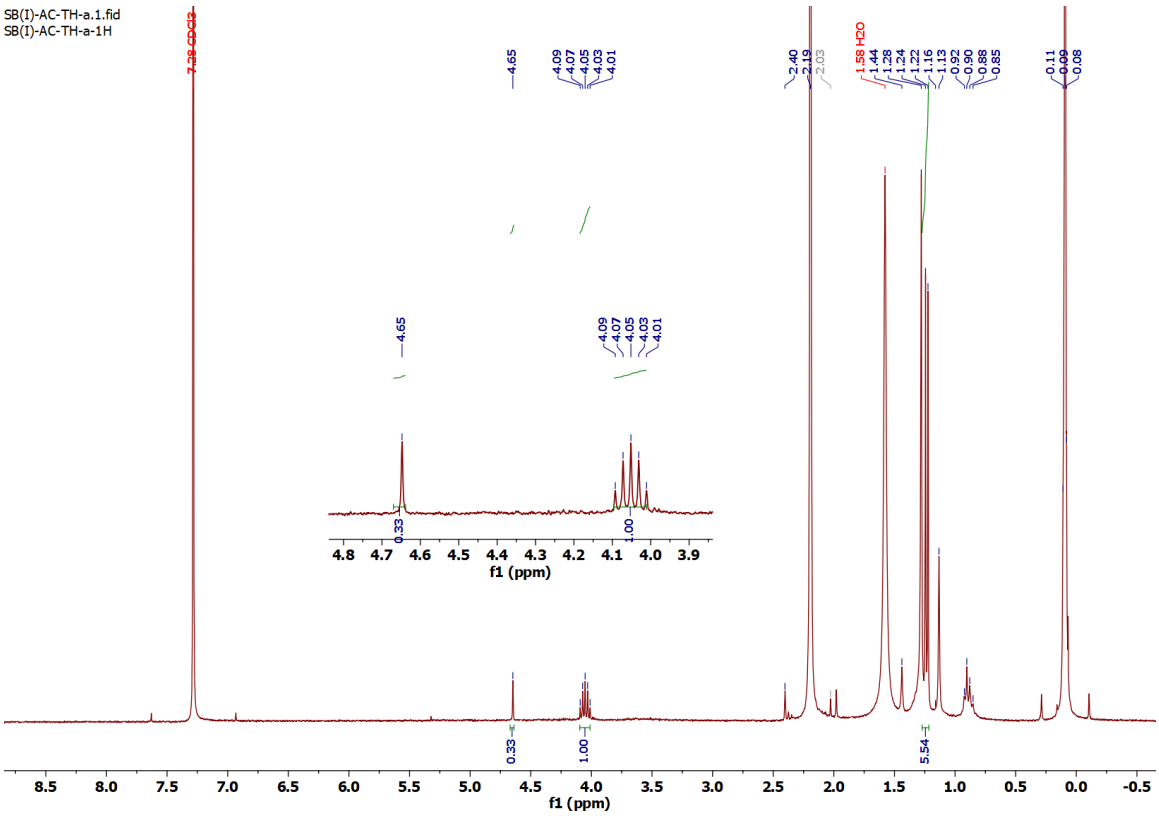

Fig. S16 ^{1}H NMR spectrum of H_2 generated from cycle-I, trapped in $CDCl_3$.

Table S19 Comparison of different catalysts for the acceptorless alcohol dehydrogenation

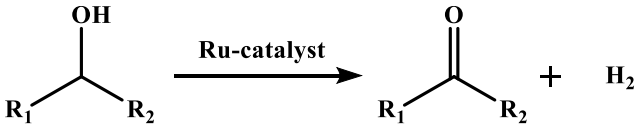

Entry	Alcohol	Ketone	TON	TOF (h^{-1})	Reference
1	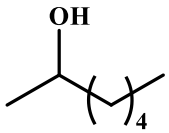	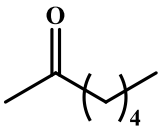	190	7.92	**25a**
2	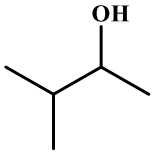	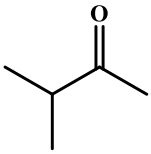	8	0.17	**25b**
3	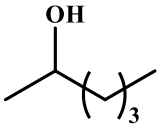	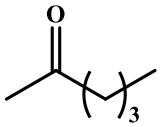	1080	24	**25c**
4	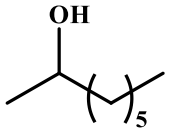	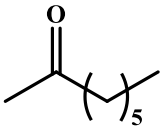	192	8	**25d**
5	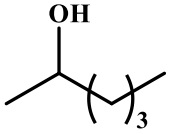	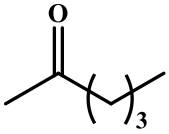	38	1.58	**25e**
6	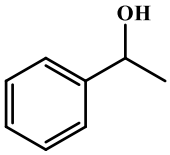	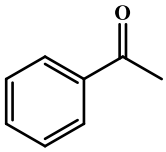	194	9.70	**25f**
7	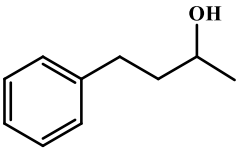	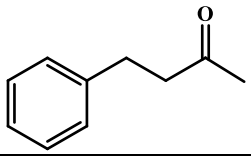	22.4	0.47	**25g**
8	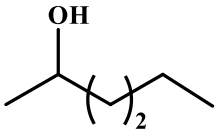	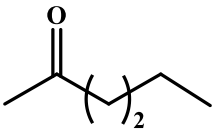	36	0.80	**25h**
9	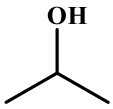	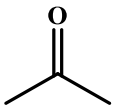	287	4.10	**25i**
10	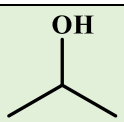	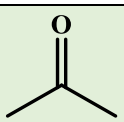	201	33.34	**This work**

Chart S1 NMR spectral characterization data for the organic products.

1,5-diphenyl-penta-1,4-(*E*,*E*)-dien-3-one (P_1). Yellow solid. Yield: 80%. ^{1}H NMR (400 MHz, $CDCl_3$): δ 7.10 (2H, d, *J* = 15.9) 7.31 – 7.49 (6H, m), 7.62 (4H, dd, *J* = 6.8, 2.9), 7.75 (2H, d, *J* = 16.0). ^{13}C{^{1}H} NMR (101 MHz, $CDCl_3$): δ 125.5, 128.5, 129.1, 130.6, 134.9, 143.4, 189.0.

1,5-Bis-(4-methoxyphenyl)-penta-1,4-(*E*,*E*)-dien-3-one (P_2). Yellow solid. Yield: 75%. ^{1}H NMR (400 MHz, $CDCl_3$): δ 3.87 (6H, s), 6.94 – 7.00 (6H, m), 7.59 (4H, d, *J* = 8.9), 7.73 (2H, d, *J* = 15.9). ^{13}C{^{1}H} NMR (101 MHz, $CDCl_3$): δ 55.4, 114.4, 123.4, 127.7, 130.1, 142.9, 161.6, 188.9.

1,5-Bis-(4-methylphenyl)-penta-1,4-(*E*,*E*)-dien-3-one (P_3). Yellow solid. Yield: 89%. ^{1}H NMR (400 MHz, $CDCl_3$): δ 2.42 (6H, s), 7.07 (2H, d, *J* = 15.9), 7.25 (4H, d, *J* = 8.1), 7.54 (4H, d, *J* = 8.1), 7.75 (2H, d, *J* = 15.9). ^{13}C{^{1}H} NMR (101 MHz, $CDCl_3$): δ 21.6, 124.6, 128.5, 129.8, 132.2, 141.0, 143.3, 189.2.

1,5-Bis-(4-fluorophenyl)-penta-1,4-(*E*,*E*)-dien-3-one (P_4). Yellow solid. Yield: 51%. ^{1}H NMR (400 MHz, $CDCl_3$): δ 7.01 (2H, d, *J* = 15.8), 7.12 (4H, m), 7.62 (4H, dd, *J* = 5.4, 3.5), 7.72 (2H, d, *J* = 15.9). ^{13}C{^{1}H} NMR (101 MHz, $CDCl_3$): δ 116.0 ($^2J_{C\text{-}F}$ = 22.2, *1st* Ar<u>C</u>H), 116.3 ($^2J_{C\text{-}F}$ = 22.2, *2nd* Ar<u>C</u>H), 126.9 ($^6J_{C\text{-}F}$ = 2.0, Ar-CH=<u>C</u>H-), 126.9 ($^6J_{C\text{-}F}$ = 2.0, Ar-CH=<u>C</u>H-), 130.3 ($^3J_{C\text{-}F}$ = 8.1, *1st* Ar<u>C</u>H), 130.3 ($^3J_{C\text{-}F}$ = 8.1, *2nd* Ar<u>C</u>H), 131.0 ($^4J_{C\text{-}F}$ = 3.0, Ar<u>C</u>), 131.0 ($^4J_{C\text{-}F}$ = 3.0, Ar<u>C</u>), 142.1 (Ar-<u>C</u>H=CH-), 162.8 ($^1J_{C\text{-}F}$ = 251.2 Ar<u>C</u>-F), 165.3 ($^1J_{C\text{-}F}$ = 251.2 Ar<u>C</u>-F), 188.5. ^{19}F NMR (377 MHz, $CDCl_3$): δ -109.5.

1,5-Bis-(4-chlorophenyl)-penta-1,4-(*E*,*E*)-dien-3-one (P_5). Yellow solid. Yield: 72%. ^{1}H NMR (400 MHz, $CDCl_3$): δ 7.05 (2H, d, *J* = 16.0), 7.42 (4H, d, *J* = 8.4), 7.57 (4H, d, *J* = 8.6), 7.71 (2H, d, *J* = 16.0). ^{13}C{^{1}H} NMR (101 MHz, $CDCl_3$): δ 125.7, 129.3, 129.5, 133.2, 136.5, 142.1, 188.3.

1,5-Bis-(4-bromophenyl)-penta-1,4-(*E*,*E*)-dien-3-one (P_6). Yellow solid. Yield: 59%. ^{1}H NMR (400 MHz, $CDCl_3$): δ 7.06 (2H, d, *J* = 16.0), 7.49 (4H, d, *J* = 8.6), 7.57 (4H, d, *J* = 8.6), 7.68 (2H, d, *J* = 15.9). ^{13}C{^{1}H} NMR (101 MHz, $CDCl_3$): δ 124.9, 125.8, 129.8, 132.3, 133.6, 142.2, 188.4.

1,5-Bis-(4-iodophenyl)-penta-1,4-(*E*,*E*)-dien-3-one (P_7). Yellow solid. Yield: 54%. ^{1}H NMR (400 MHz, $CDCl_3$): δ 7.07 (2H, d, *J* = 15.9), 7.35 (4H, dd, *J* = 8.3, 2.0), 7.66 (2H, d, *J* = 15.9), 7.78 (4H, dd, *J* = 7.6, 2.2). ^{13}C{^{1}H} NMR (101 MHz, $CDCl_3$): δ 96.8, 125.9, 129.7, 134.2, 138.2, 142.1, 188.3.

1,5-Bis-(2-methoxyphenyl)-penta-1,4-(*E*,*E*)-dien-3-one (P_8). Yellow solid. Yield: 81%. ^{1}H NMR (400 MHz, $CDCl_3$): δ 3.93 (6H, s), 6.95 (2H, dd, *J* = 8.5, 1.1), 7.01 (2H, td, *J* = 7.5, 1.1), 7.20 (2H, d, *J* = 16.1), 7.39 (2H, m), 7.64 (2H, dd, *J* = 7.7, 1.8), 8.09 (2H, d, *J* = 16.2). ^{13}C{^{1}H} NMR (101 MHz, $CDCl_3$): δ 55.6, 111.2, 120.8, 124.0, 126.2, 128.7, 131.6, 138.3, 158.6, 190.1.

1,5-Bis-(2-fluorophenyl)-penta-1,4-(*E*,*E*)-dien-3-one (P_9). Yellow solid. Yield: 48%. ^{1}H NMR (400 MHz, $CDCl_3$): δ 7.11 – 7.20 (6H, m), 7.29 – 7.34 (2H, m), 7.64 (2H, dt, *J* = 7.6, 1.9), 7.84 (2H, d, *J* = 16.1). ^{13}C{^{1}H} NMR (101 MHz, $CDCl_3$): δ 116.1 ($^2J_{C\text{-}F}$ = 21.9, *1st* Ar<u>*C*</u>H), 116.3 ($^2J_{C\text{-}F}$ = 21.9, *2nd* Ar<u>*C*</u>H), 122.7 ($^2J_{C\text{-}F}$ = 11.7, ArC), 122.8 ($^2J_{C\text{-}F}$ = 11.7, ArC), 124.5 ($^3J_{C\text{-}F}$ = 3.6, Ar-CH=<u>*C*</u>H-), 124.6 ($^3J_{C\text{-}F}$ = 3.6, Ar-CH=<u>*C*</u>H-), 127.5 ($^3J_{C\text{-}F}$ = 6.2, *1st* Ar<u>*C*</u>H), 127.6 ($^3J_{C\text{-}F}$ = 6.2, *2nd* Ar<u>*C*</u>H), 129.3 ($^3J_{C\text{-}F}$ = 2.9, *1st* Ar<u>*C*</u>H), 129.3 ($^3J_{C\text{-}F}$ = 2.9, *2nd* Ar<u>*C*</u>H), 131.9 ($^4J_{C\text{-}F}$ = 8.7, *1st* Ar<u>*CH*</u>), 132.0 ($^4J_{C\text{-}F}$ = 8.7, *2nd* Ar<u>*CH*</u>), 135.9 (Ar-<u>*C*</u>H=CH-), 160.3 ($^1J_{C\text{-}F}$ = 254.8 Ar<u>*C*</u>-F), 162.8 ($^1J_{C\text{-}F}$ = 254.8 Ar<u>*C*</u>-F), 188.7. ^{19}F NMR (377 MHz, $CDCl_3$): δ -114.7.

1,5-Bis-(2-nitrophenyl)-penta-1,4-(*E*,*E*)-dien-3-one (P_{10}). Yellow solid. Yield: 57%. ^{1}H NMR (400 MHz, $CDCl_3$): δ 7.00 (2H, d, *J* = 16.0), 7.60 (2H, ddd, *J* = 8.6, 6.9, 1.9), 7.70 – 7.77 (4H, m), 8.10 (2H, dd, *J* = 8.1, 1.4), 8.18 (2H, d, *J* = 15.9). ^{13}C{^{1}H} NMR (101 MHz, $CDCl_3$): δ 125.1, 129.2, 130.6, 131.0, 139.4, 148.5, 188.3.

1,5-Bis-(3-nitrophenyl)-penta-1,4-(*E*,*E*)-dien-3-one (P_{11}). Brown solid. Yield: 93%. ^{1}H NMR (400 MHz, DMSO-d_6): δ 7.58 (2H, d, *J* = 16.1), 7.78 (2H, t, *J* = 7.8), 7.97 (2H, d, *J* = 16.1), 8.27 – 8.33 (4H, m), 8.65 (2H, t, *J* = 2.0). ^{13}C{^{1}H} NMR (101 MHz, DMSO-d_6): δ 123.4, 125.2, 128.4, 131.0, 135.0, 137.0, 141.3, 148.9, 189.0.

1,5-Bis-(2,5-dimethoxyphenyl)-penta-1,4-(*E*,*E*)-dien-3-one (P_{12}). Yellow solid. Yield: 73%. ^{1}H NMR (400 MHz, $CDCl_3$): δ 3.88 (6H, s), 3.93 (6H, s), 6.88 – 7.01 (4H, m), 7.14 – 7.19 (4H, m), 8.03 (2H, d, *J* = 16.2). ^{13}C{^{1}H} NMR (101 MHz, $CDCl_3$): δ 55.6, 55.8, 111.3, 112.0, 117.2, 124.4, 127.5, 136.6, 152.9, 153.5, 189.6.

1,5-Bis-(2,6-dichlorophenyl)-penta-1,4-(*E*,*E*)-dien-3-one (P_{13}). Yellow solid. Yield: 65%. ^{1}H NMR (400 MHz, DMSO-d_6): δ 7.28 (2H, d, *J* = 16.4), 7.44 (2H, dd, *J* = 7.5, 1.2), 7.59 (4H, d, *J* = 8.4), 7.74 (2H, d, *J* = 16.4). ^{13}C{^{1}H} NMR (101 MHz, DMSO-d_6): δ 129.6, 131.6, 132.3, 133.7, 134.5, 137.4, 188.5.

1,5-Bis-(naphthalen-1-yl)-penta-1,4-(*E*,*E*)-dien-3-one (P_{14}). Yellow solid. Yield: 71%. ^{1}H NMR (400 MHz, $CDCl_3$): δ 7.27 (2H, d, *J* = 15.6), 7.56 – 7.66 (6H, m), 7.92 – 7.97 (6H, m), 8.31 (2H, d, *J* = 8.6), 8.68 (2H, d, *J* = 15.8). ^{13}C{^{1}H} NMR (101 MHz, $CDCl_3$): δ 123.5, 125.2, 125.5, 126.3, 127.0, 128.1, 128.9, 130.8, 131.8, 132.3, 133.8, 140.4, 188.7.

1,5-Bis-(anthracen-9-yl)-penta-1,4-(*E*,*E*)-dien-3-one (P_{15}). Yellow solid. Yield: 66%. ^{1}H NMR (400 MHz, $CDCl_3$): δ 7.21 (2H, d, *J* = 16.2), 7.50 – 7.57 (8H, m), 8.05 (4H, d, *J* = 8.1), 8.35 (4H, d, *J* = 8.5), 8.50 (2H, s), 8.82 (2H, d, *J* = 16.1). ^{13}C{^{1}H} NMR (101 MHz, $CDCl_3$): δ 123.5, 125.7, 129.1, 129.3, 131.0, 132.1, 135.2, 148.5, 192.9.

(1E,3E,6E,8E)-1,9-diphenylnona-1,3,6,8-tetraen-5-one (P_{16}). Yellow solid. Yield: 67%. ^{1}H NMR (400 MHz, $CDCl_3$): δ 6.60 (2H, d, *J* = 15.1), 6.94 – 7.02 (4H, m), 7.33 – 7.43 (6H, m), 7.47 – 7.55 (6H, m). ^{13}C{^{1}H} NMR (101 MHz, $CDCl_3$): δ 127.0, 127.3, 128.9, 129.1, 129.2, 136.2, 141.5, 143.1, 189.0.

1,5-Bis-(4-cyanophenyl)-penta-1,4-(*E*,*E*)-dien-3-one (P_{17}). Yield: 0%.

1,5-Bis-(4-(dimethylamino)phenyl)-penta-1,4-(*E*,*E*)-dien-3-one (P_{18}). Red solid. Yield: 77%. ^{1}H NMR (400 MHz, $CDCl_3$): δ 3.05 (12H, s), 6.71 (4H, d, *J* = 9.0), 6.91 (2H, d, *J* = 15.7), 7.54 (4H, d, *J* = 9.0), 7.71 (2H, d, *J* = 15.7). ^{13}C{^{1}H} NMR (101 MHz, $CDCl_3$): δ 40.2, 111.9, 121.4, 123.0, 130.1, 143.0, 151.8, 188.9.

1,5-Bis-(pyridin-2-yl)-penta-1,4-(*E*,*E*)-dien-3-one (P_{19}). Yellow solid. Yield: 26%. ^{1}H NMR (400 MHz, CD_3OD): δ 7.44 (2H, dd, *J* = 8.4, 5.2), 7.61 (2H, d, *J* = 15.9), 7.75 – 7.80 (4H, m), 7.90 (2H, td, *J* = 7.8, 2.5), 8.63 (2H, d, *J* = 4.7). ^{13}C{^{1}H} NMR (101 MHz, DMSO-d_6): δ 124.3, 131.9, 137.6, 141.2, 148.6, 150.8, 155.7, 188.0.

1,5-Bis-(2-hydroxyphenyl)-penta-1,4-(*E*,*E*)-dien-3-one (P_{20}). Yellow solid. Yield: 56%. ^{1}H NMR (400 MHz, $CDCl_3$): δ 6.85 (2H, t, *J* = 7.4), 6.95 (2H, d, *J* = 8.4), 7.24 –

7.30 (4H, m), 7.69 (2H, dd, *J* = 8.2, 1.6), 7.92 (2H, d, *J* = 16.0). $^{13}C\{^{1}H\}$ NMR (101 MHz, $CDCl_3$): δ 116.9, 120.0, 121.9, 125.9, 129.3, 138.5, 157.7, 189.2.

1,5-Bis-(pyrrol-2-yl)-penta-1,4-(*E*,*E*)-dien-3-one (P_{21}). Yield: 0%.

1,5-Bis-(2-hydroxynaphthalen-1-yl)-penta-1,4-(*E*,*E*)-dien-3-one (P_{22}). Yield: 0%.

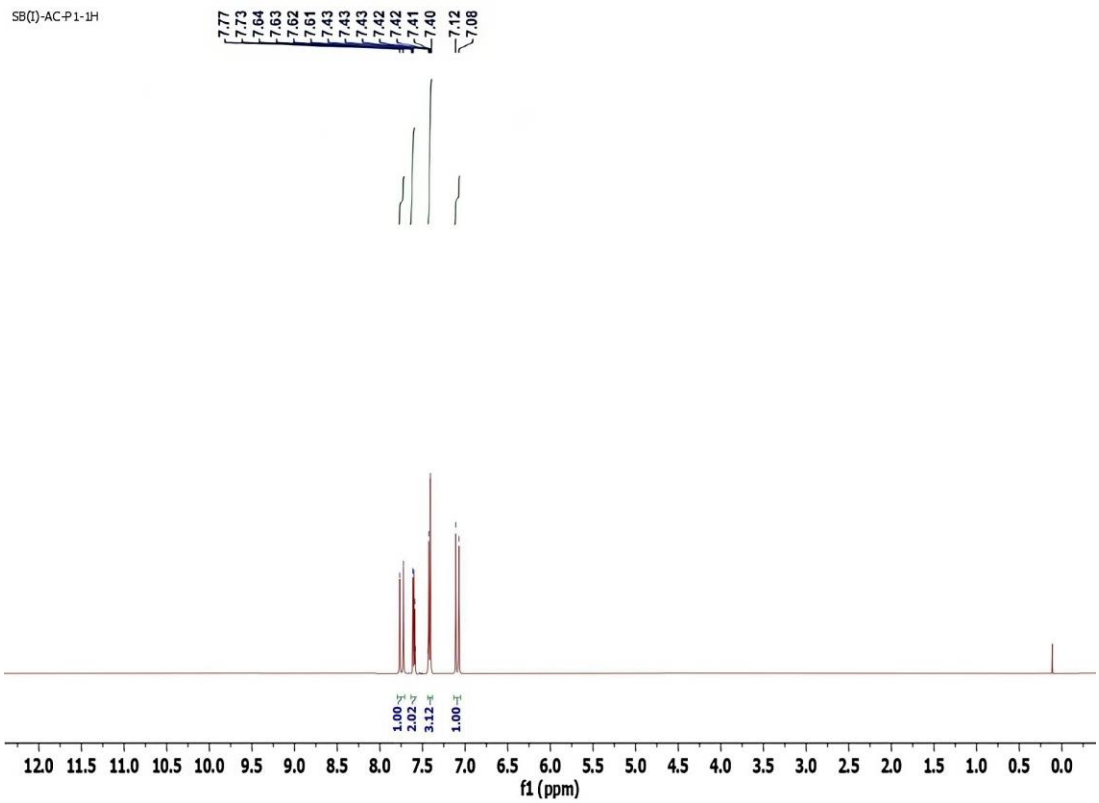

^{1}H NMR spectrum of **P₁** in $CDCl_3$

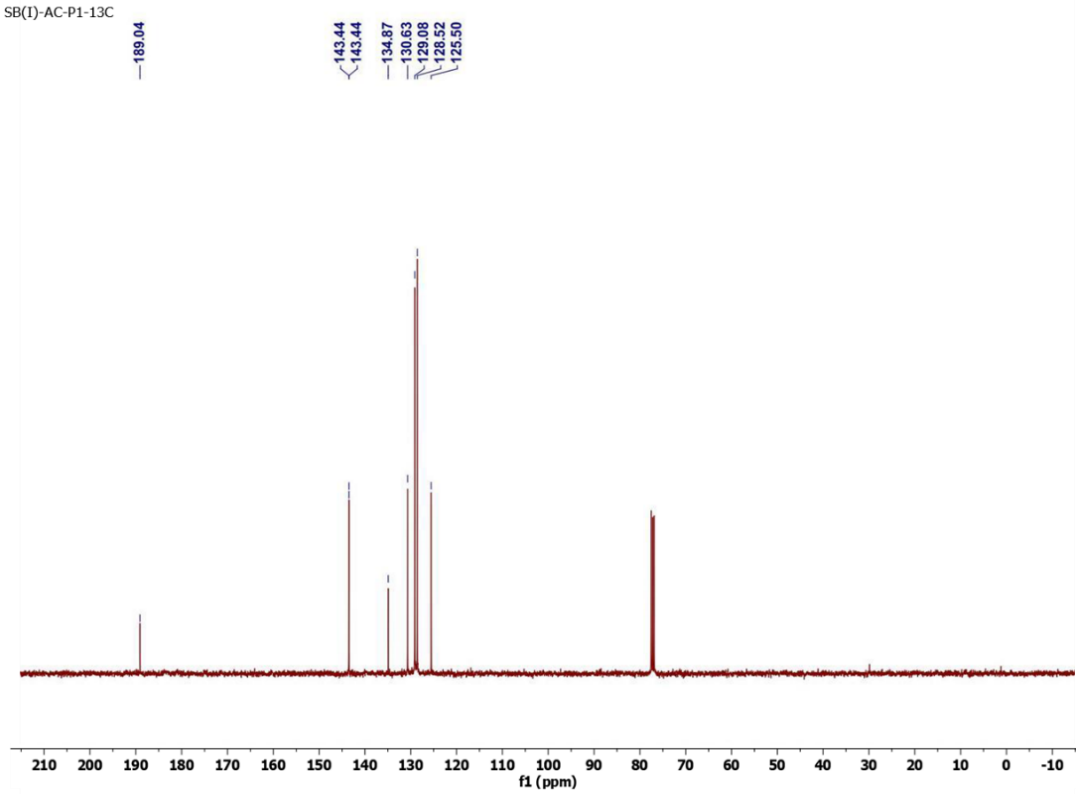

^{13}C NMR spectrum of **P₁** in $CDCl_3$

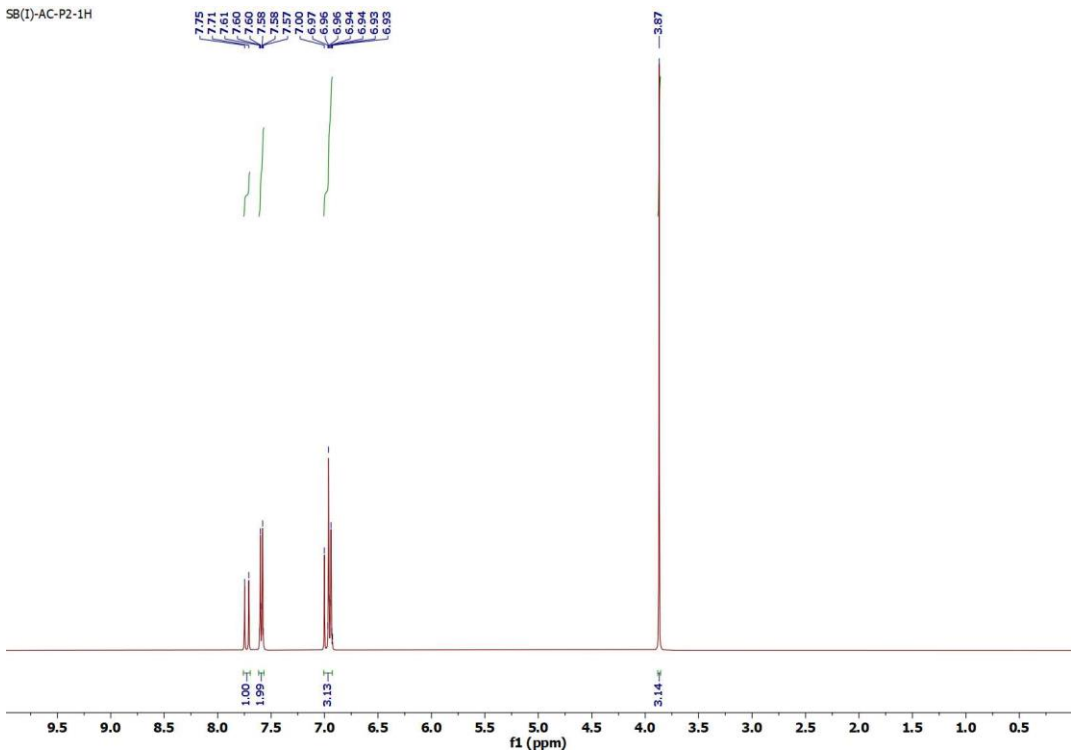

^{1}H NMR spectrum of **P2** in $CDCl_3$

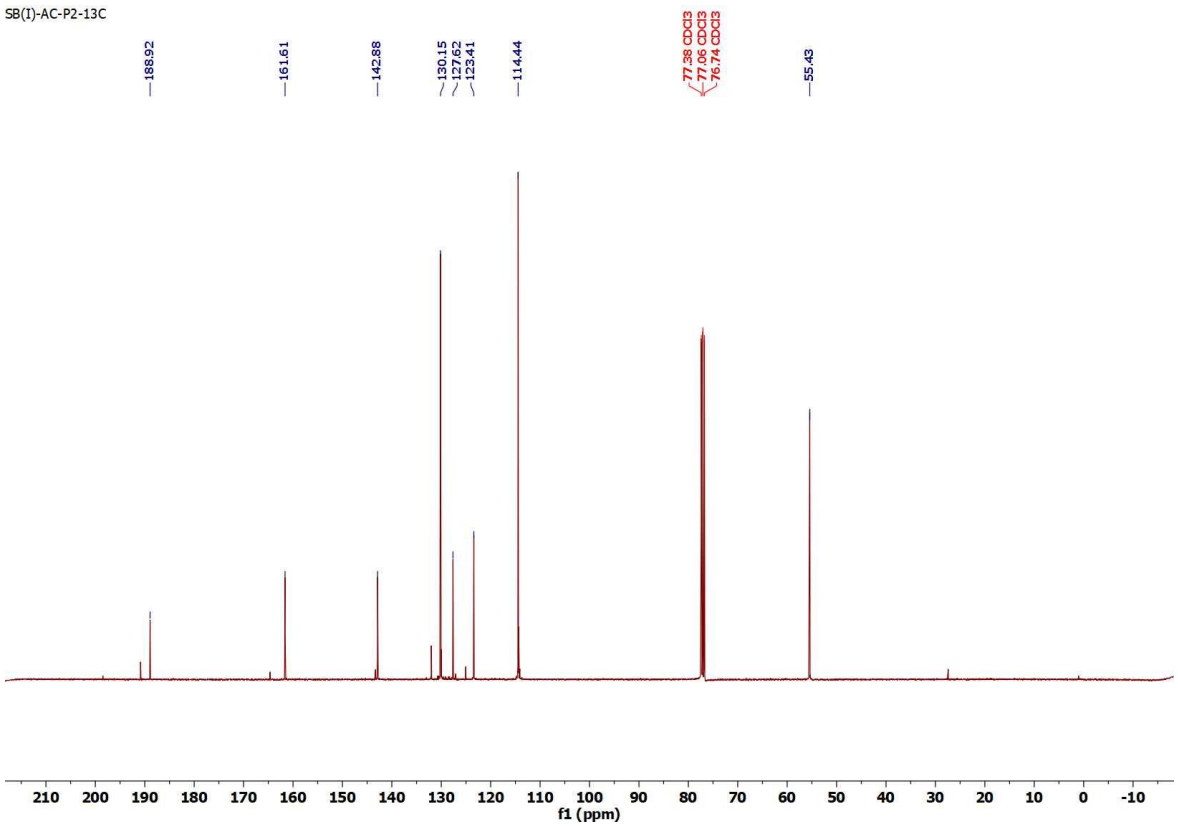

^{13}C NMR spectrum of **P2** in $CDCl_3$

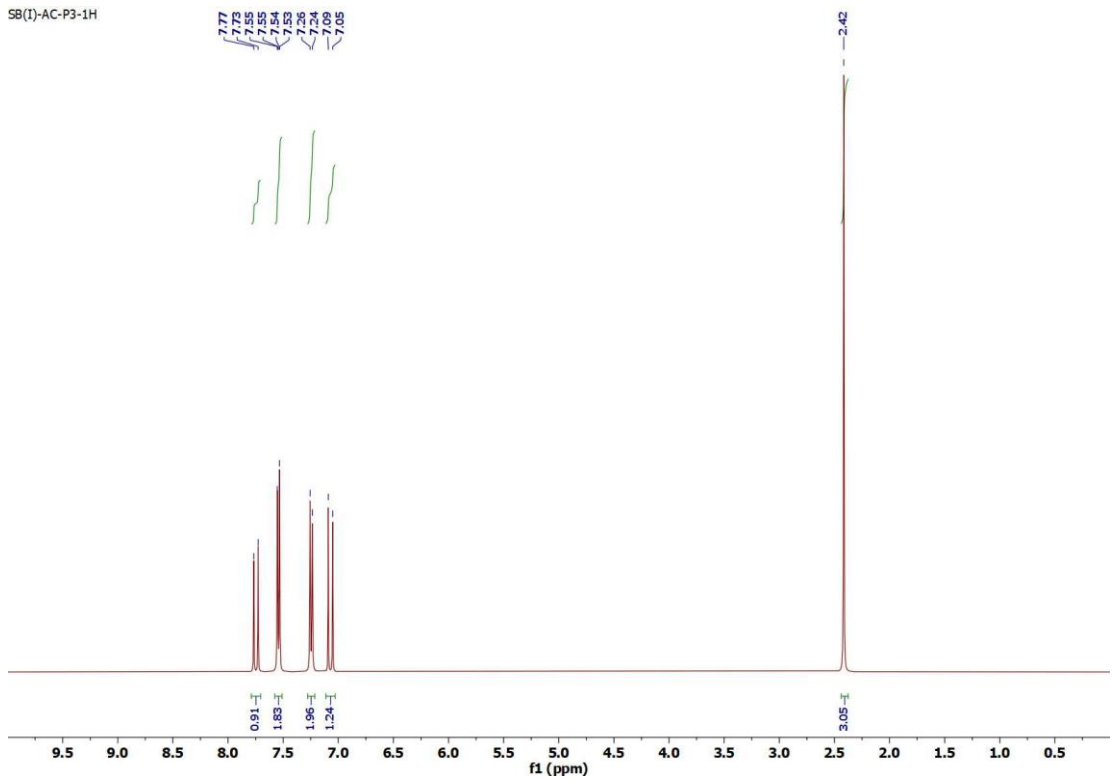

^{1}H NMR spectrum of **P3** in $CDCl_3$

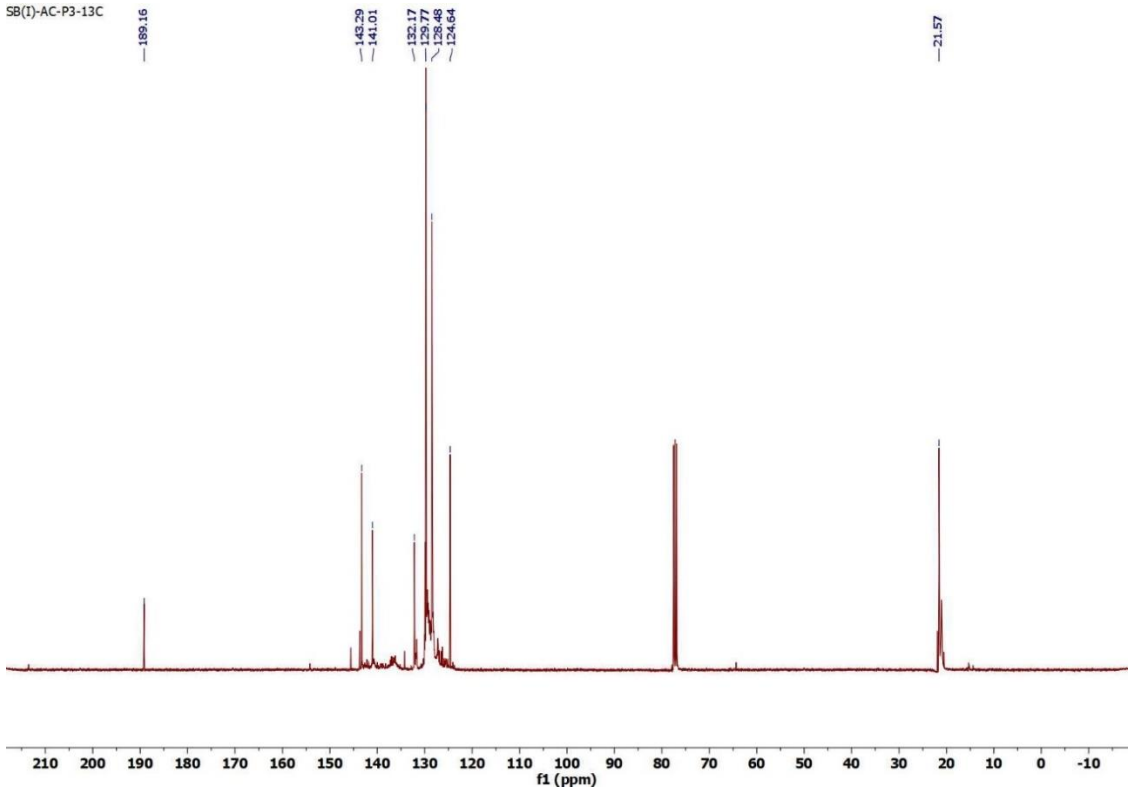

^{13}C NMR spectrum of **P3** in $CDCl_3$

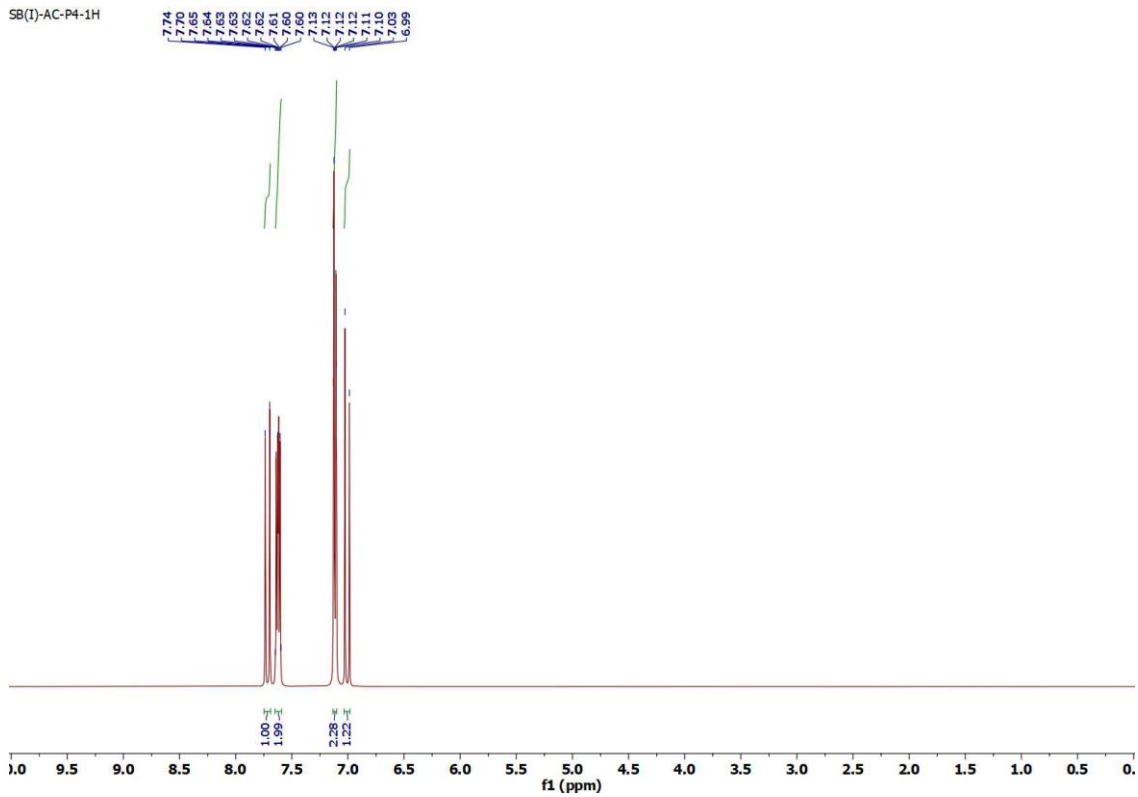

^{1}H NMR spectrum of **P4** in $CDCl_3$

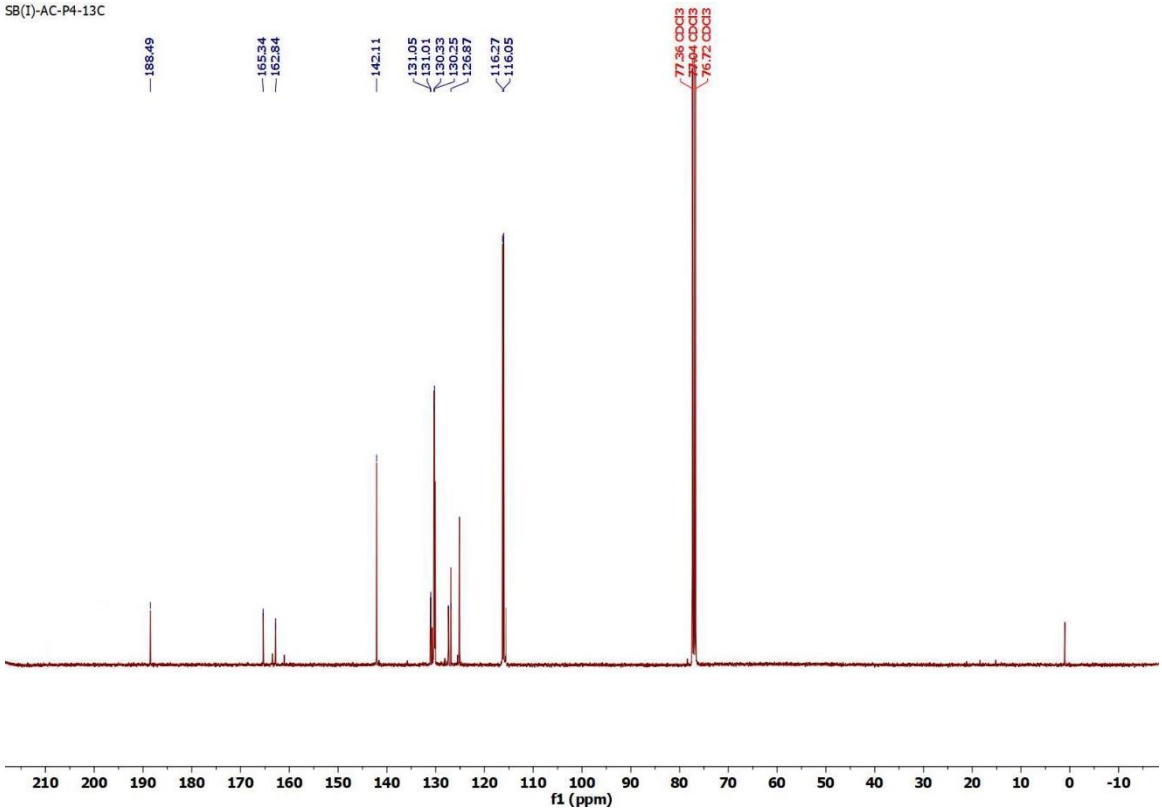

^{13}C NMR spectrum of **P4** in $CDCl_3$

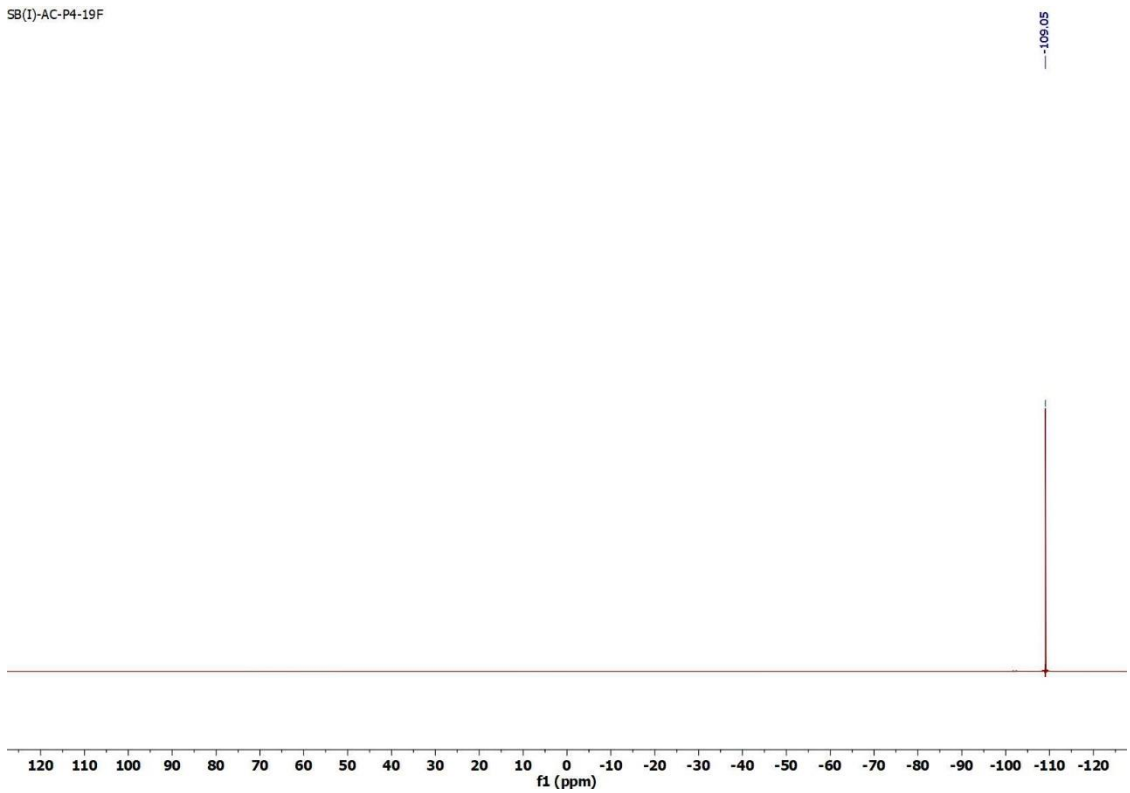

^{19}F NMR spectrum of **P₄** in $CDCl_3$

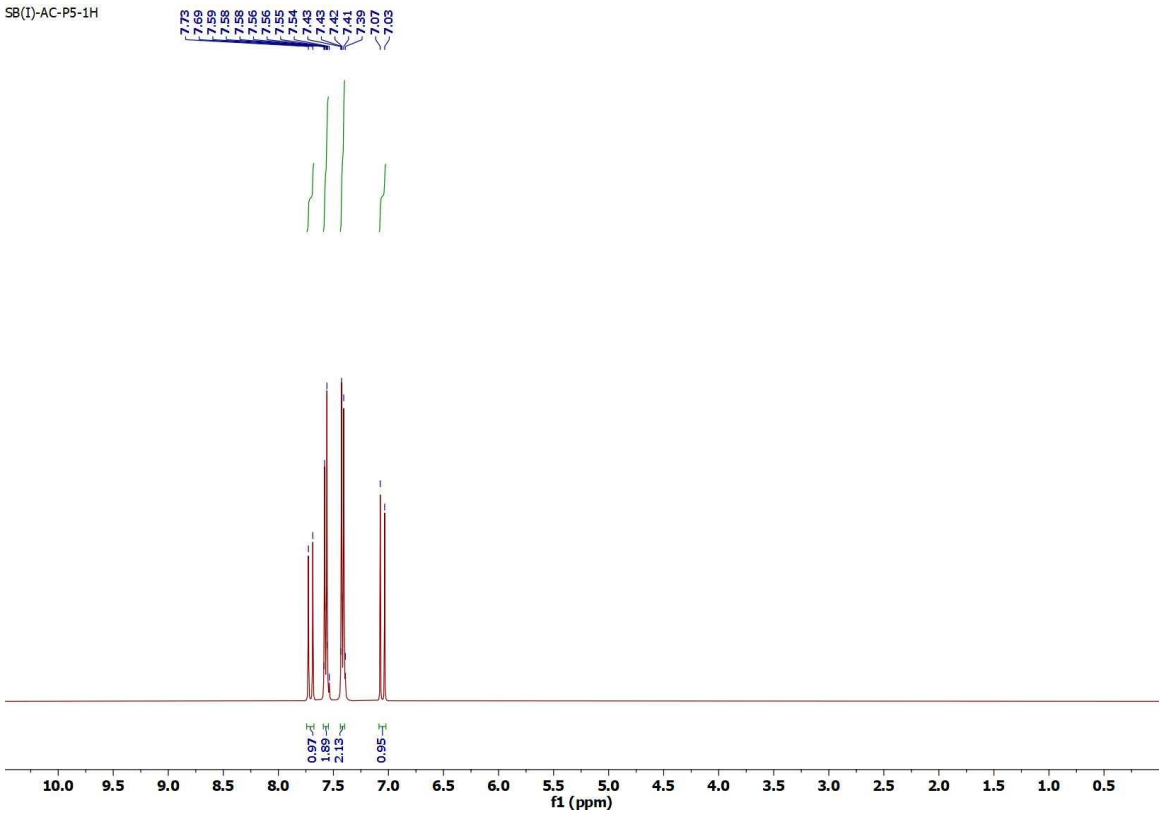

^{1}H NMR spectrum of **P₅** in $CDCl_3$

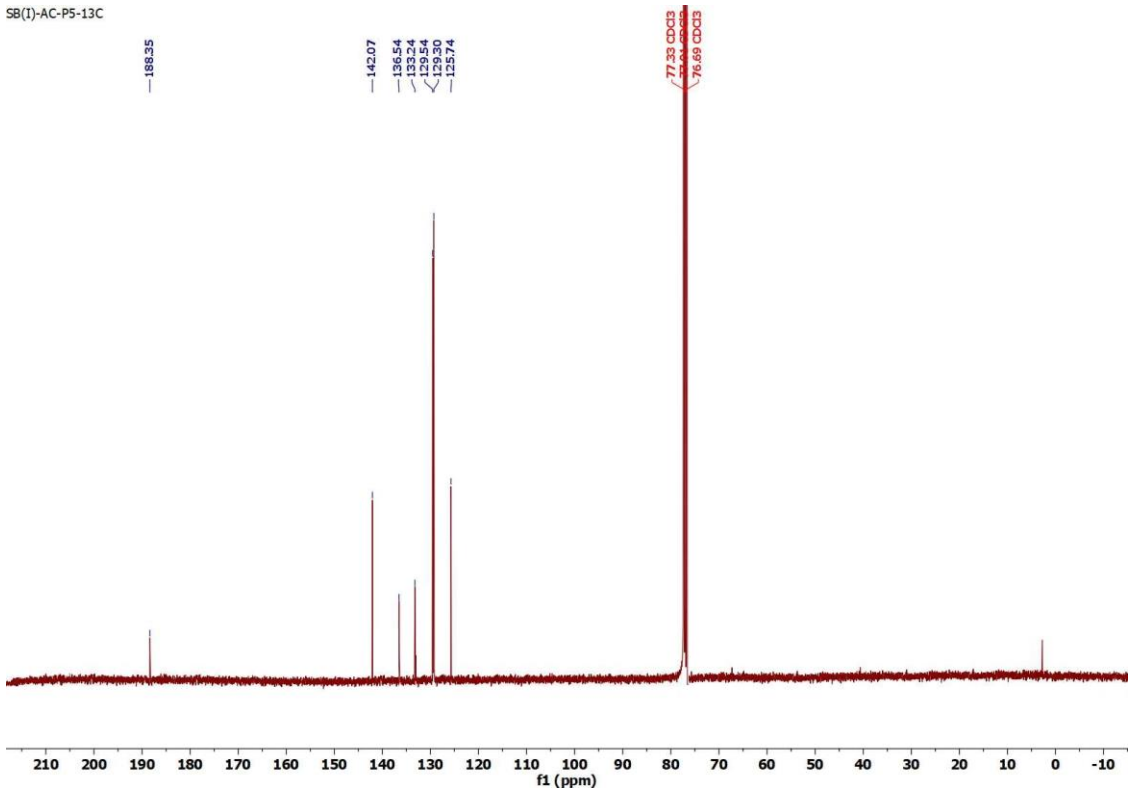

^{13}C NMR spectrum of **P5** in $CDCl_3$

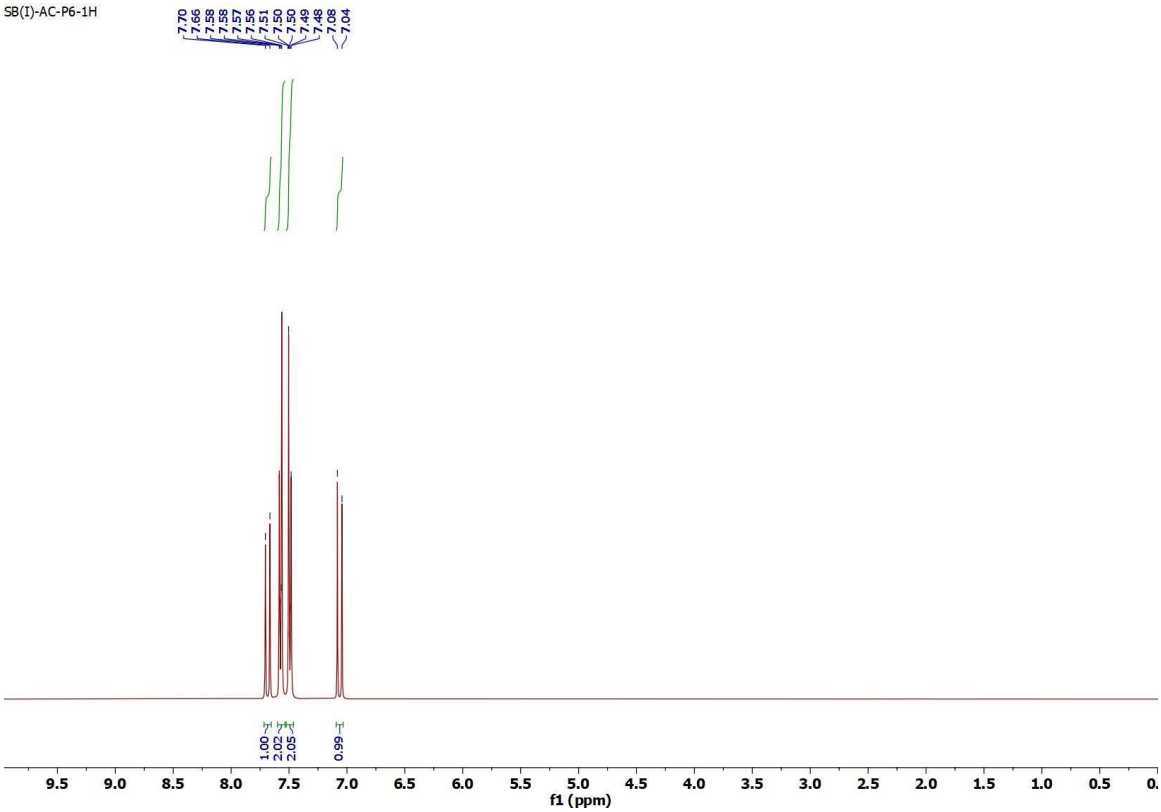

^{1}H NMR spectrum of **P6** in $CDCl_3$

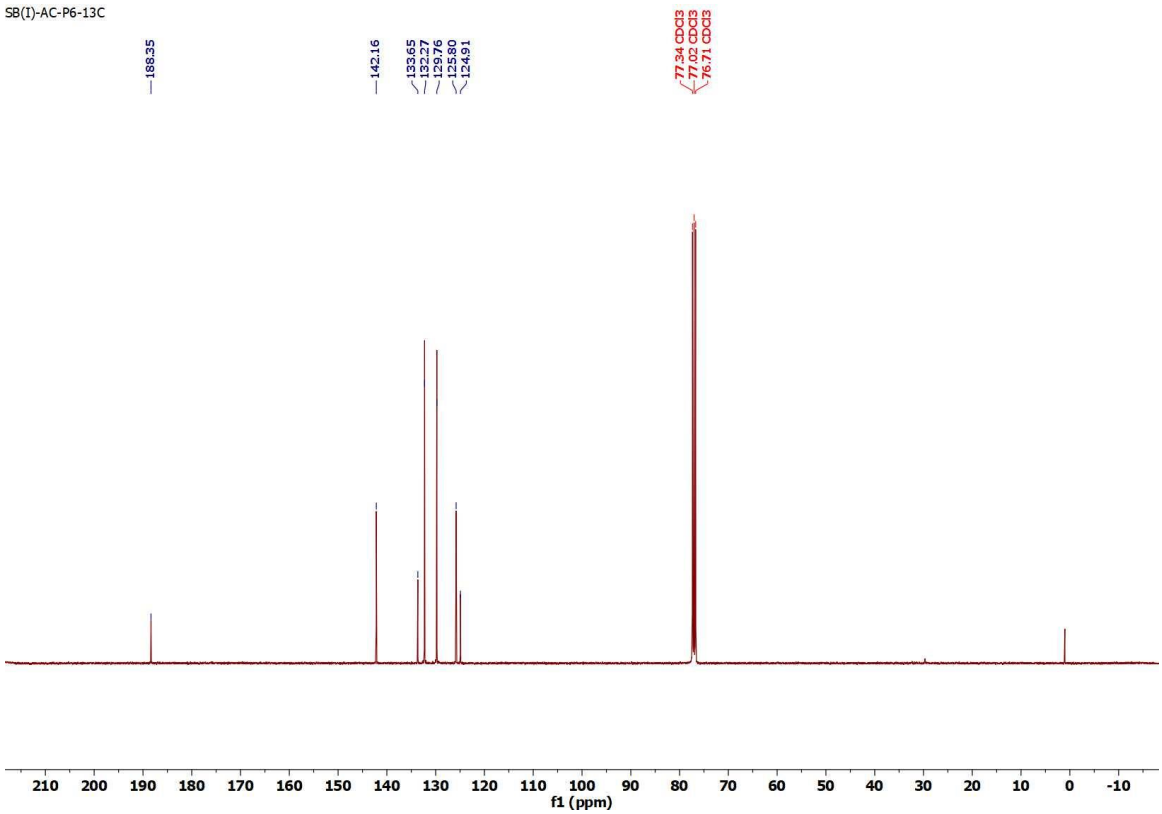

^{13}C NMR spectrum of **P$_6$** in $CDCl_3$

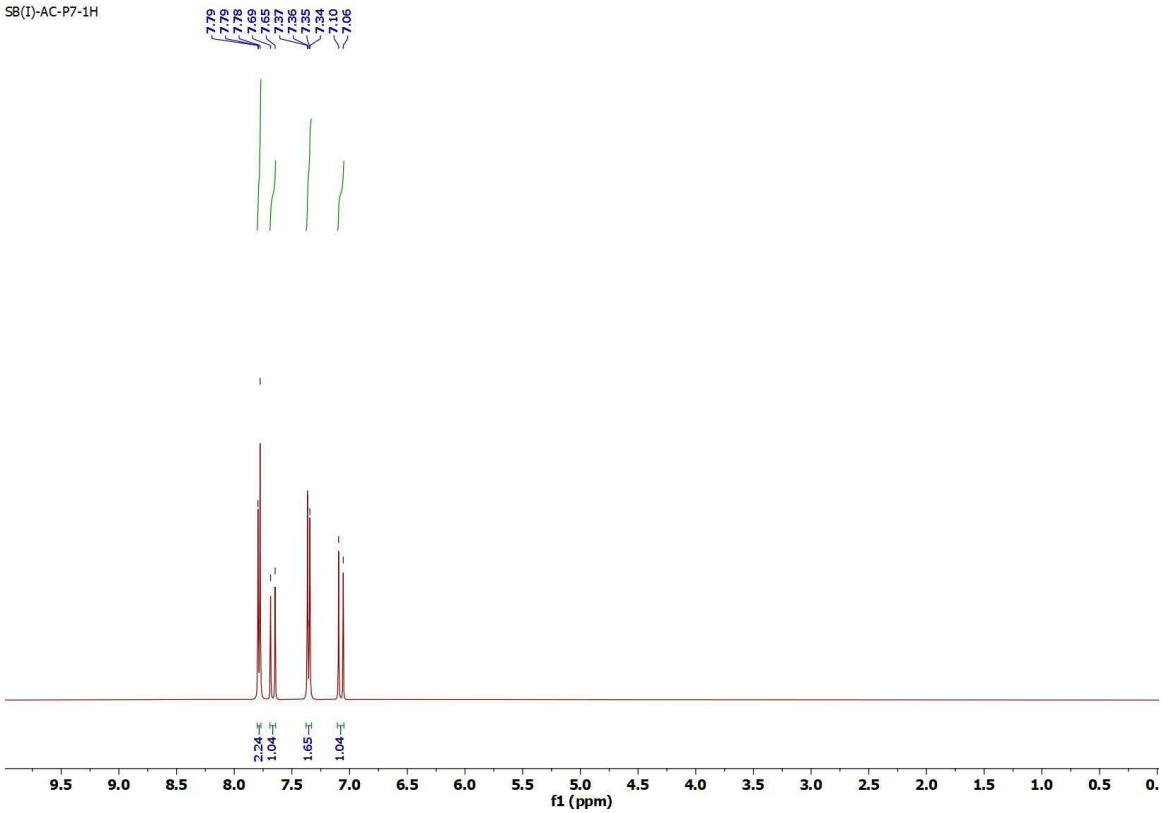

^{1}H NMR spectrum of **P$_7$** in $CDCl_3$

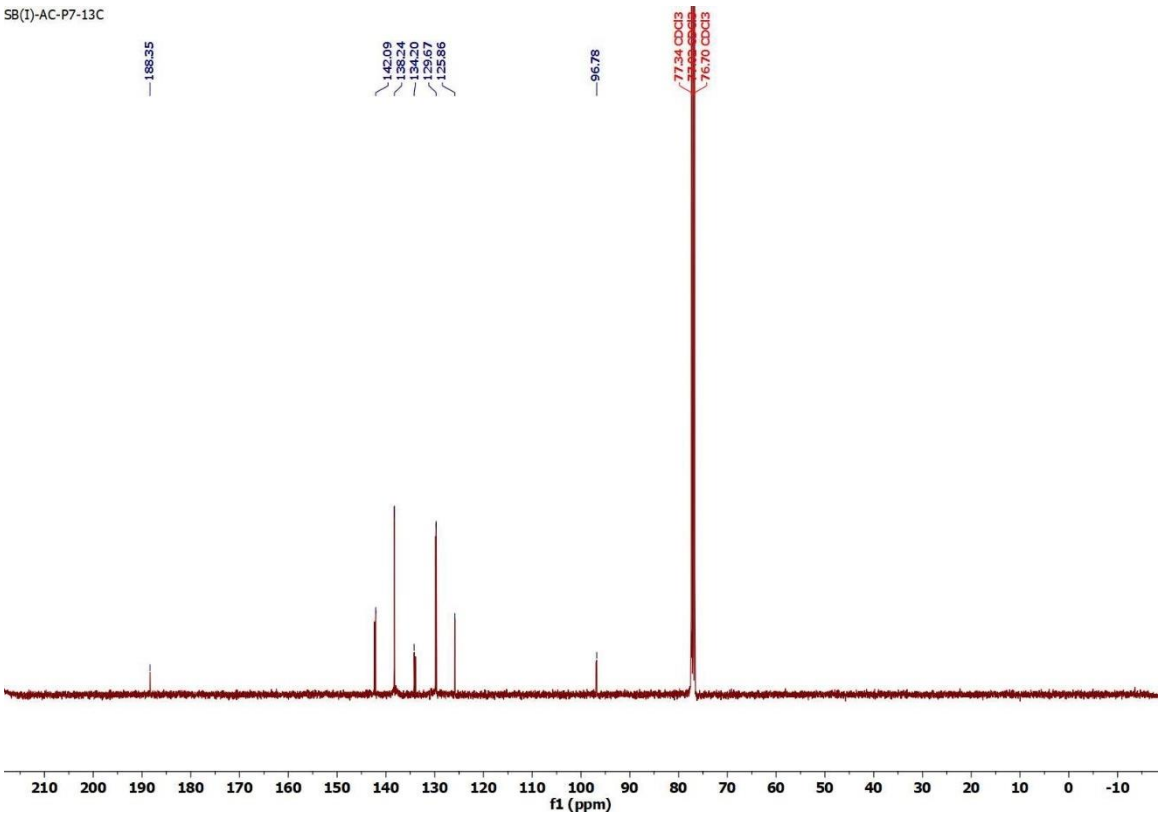

^{13}C NMR spectrum of **P7** in $CDCl_3$

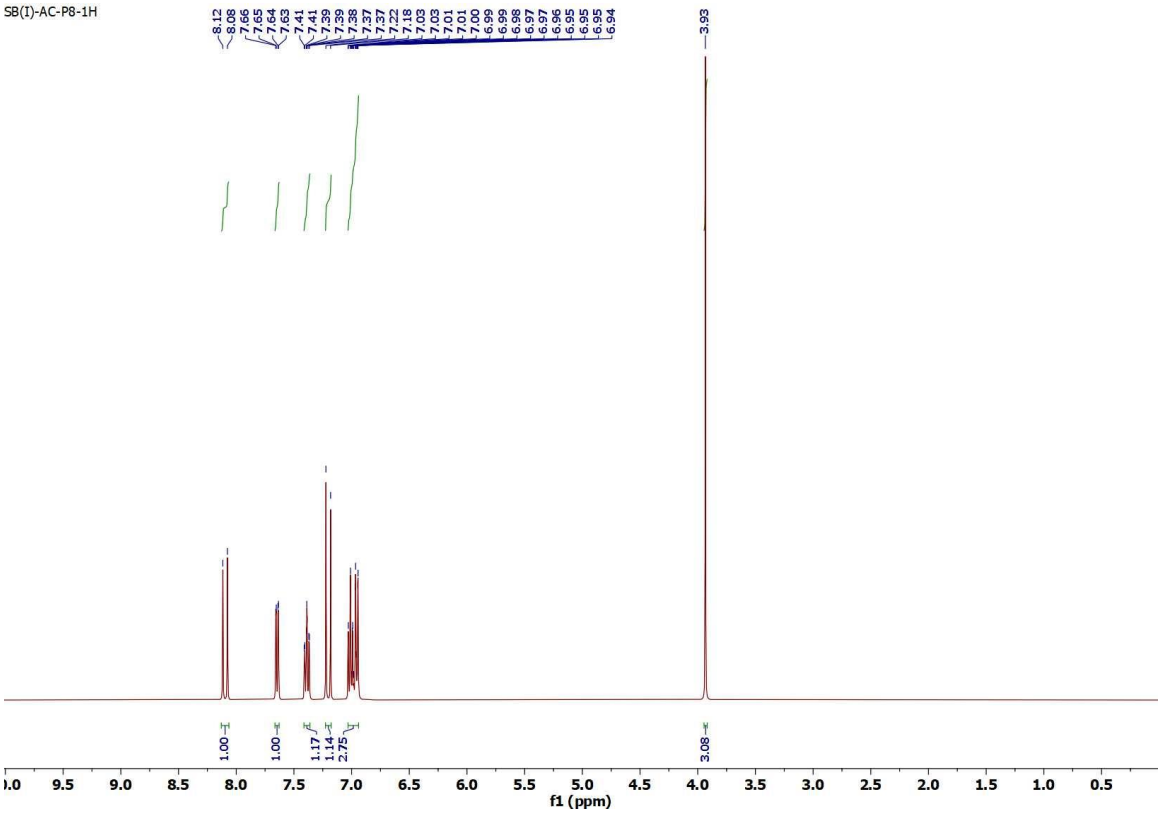

^{1}H NMR spectrum of **P8** in $CDCl_3$

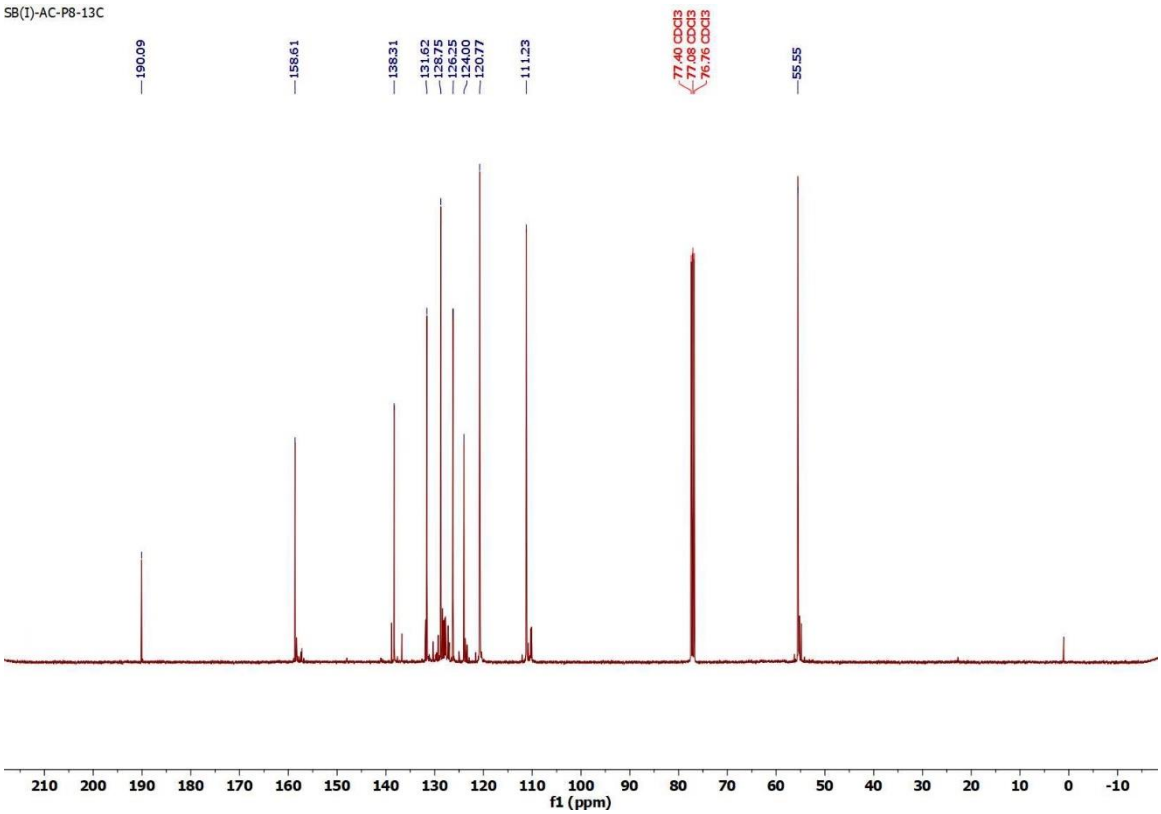

^{13}C NMR spectrum of **P8** in $CDCl_3$

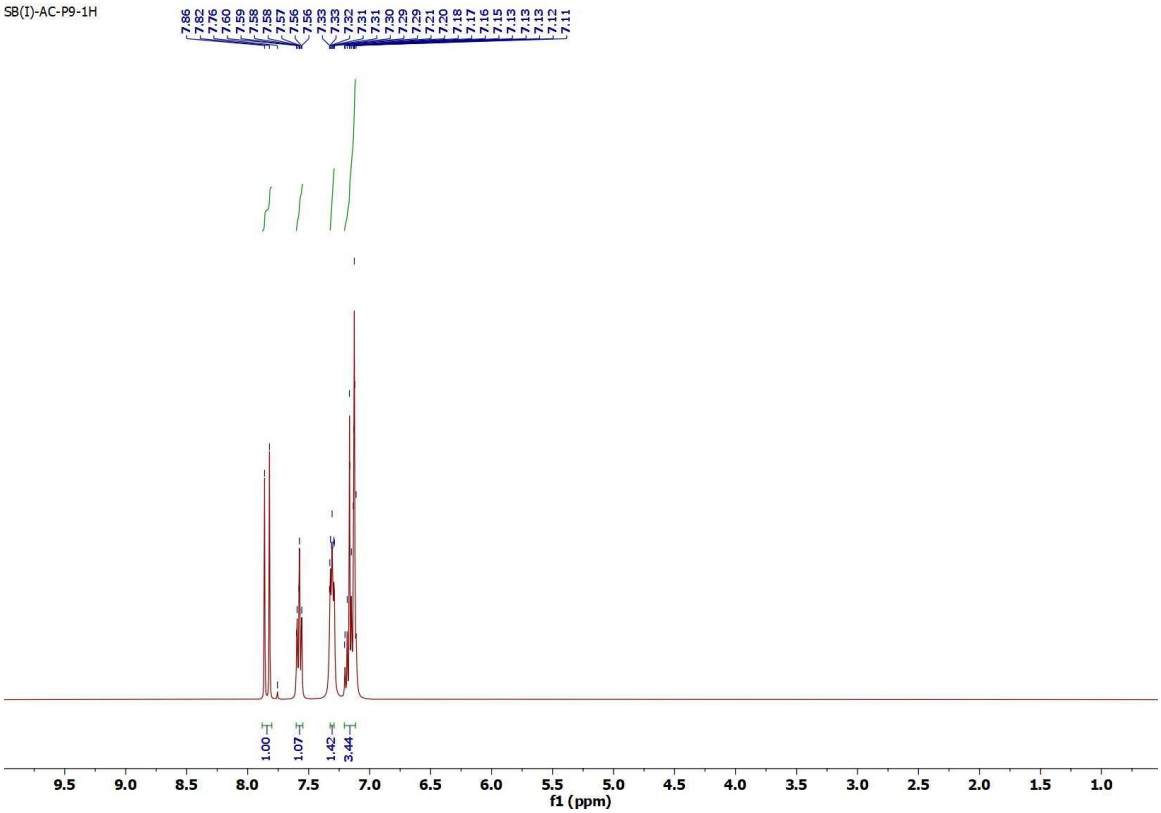

^{1}H NMR spectrum of **P9** in $CDCl_3$

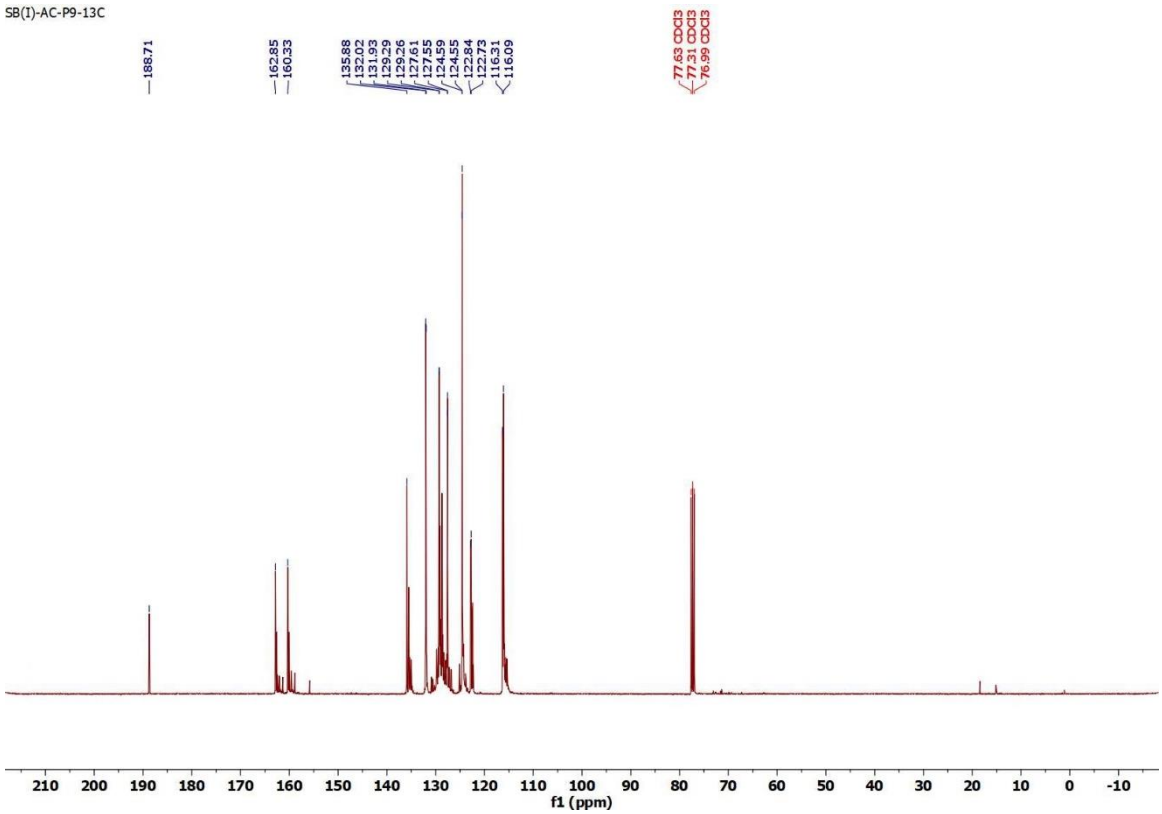

^{13}C NMR spectrum of **P9** in $CDCl_3$

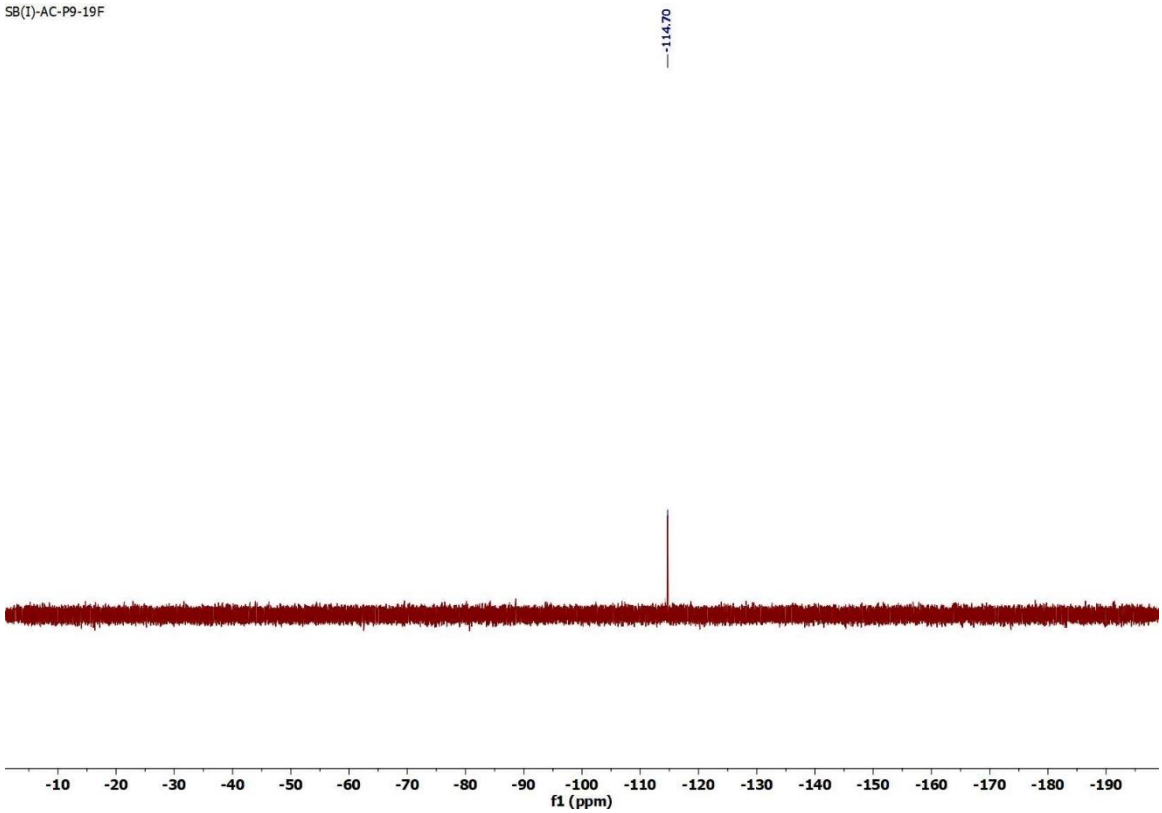

^{19}F NMR spectrum of **P9** in $CDCl_3$

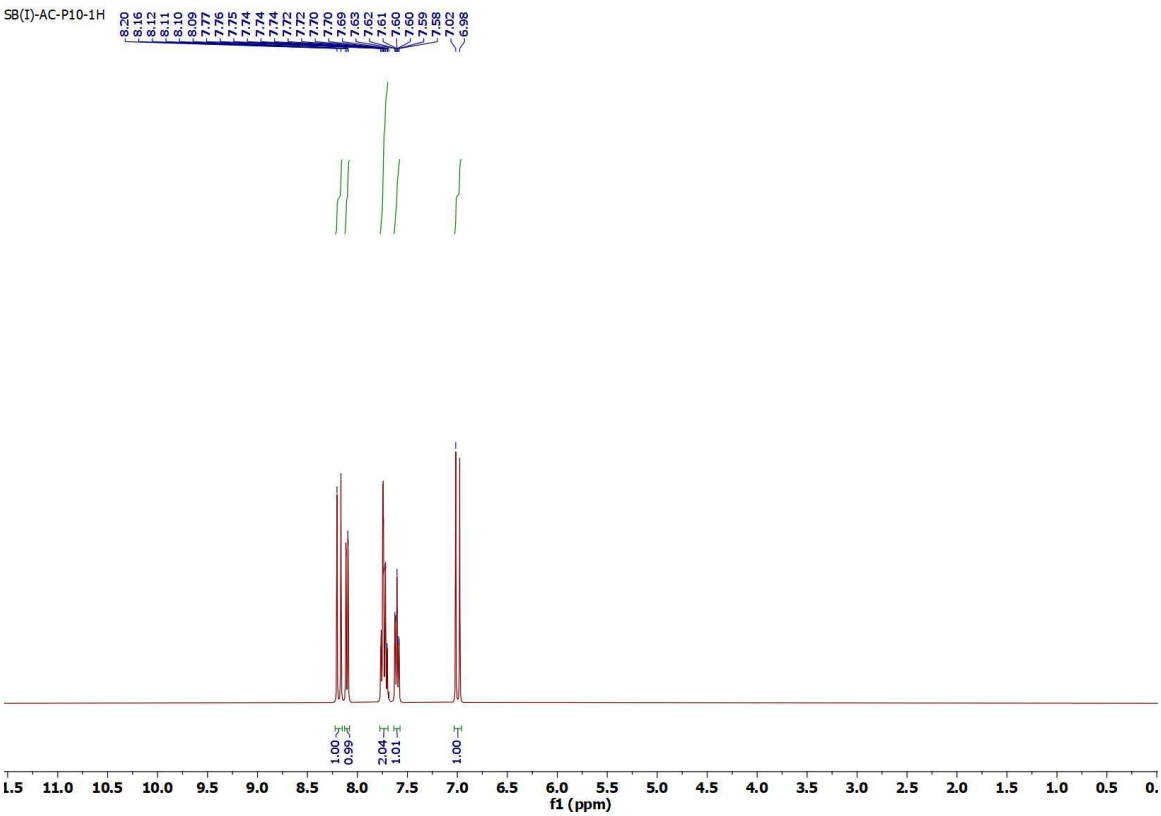

^{1}H NMR spectrum of **P_{10}** in $CDCl_3$

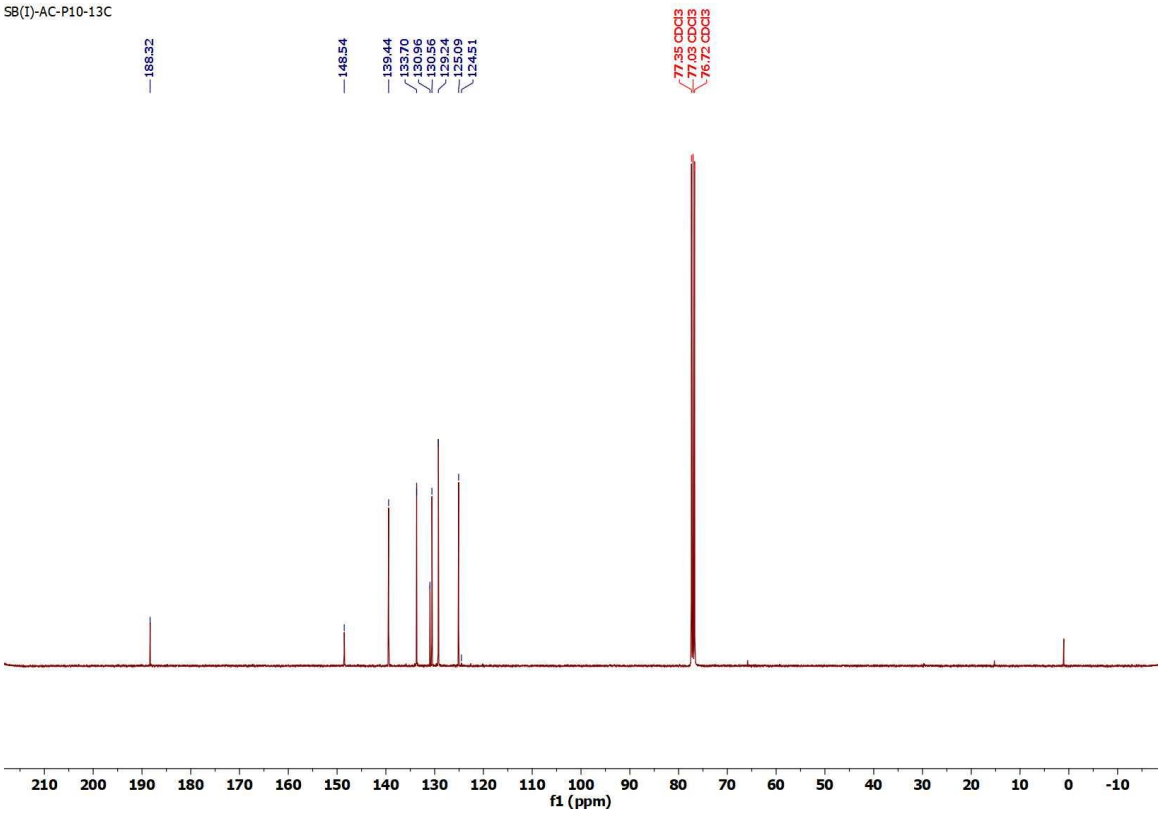

^{13}C NMR spectrum of **P_{10}** in $CDCl_3$

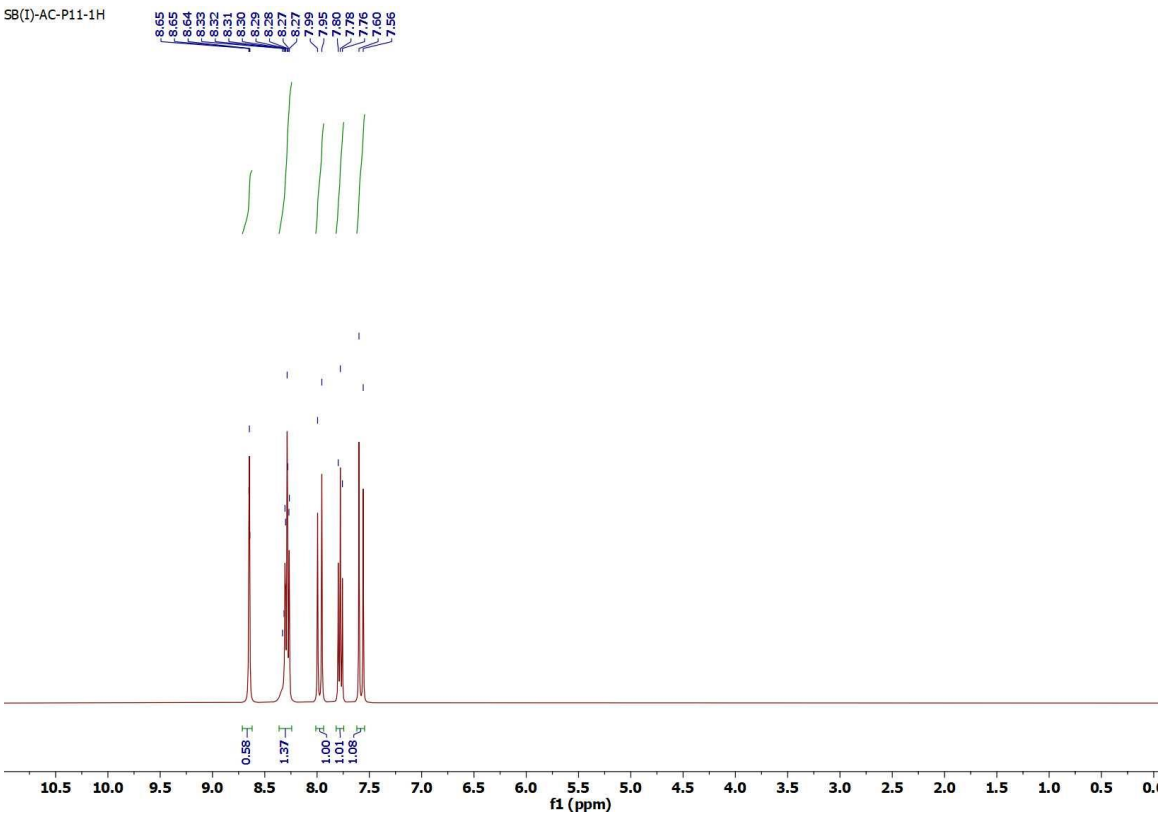

^{1}H NMR spectrum of **P$_{11}$** in DMSO-d$_6$

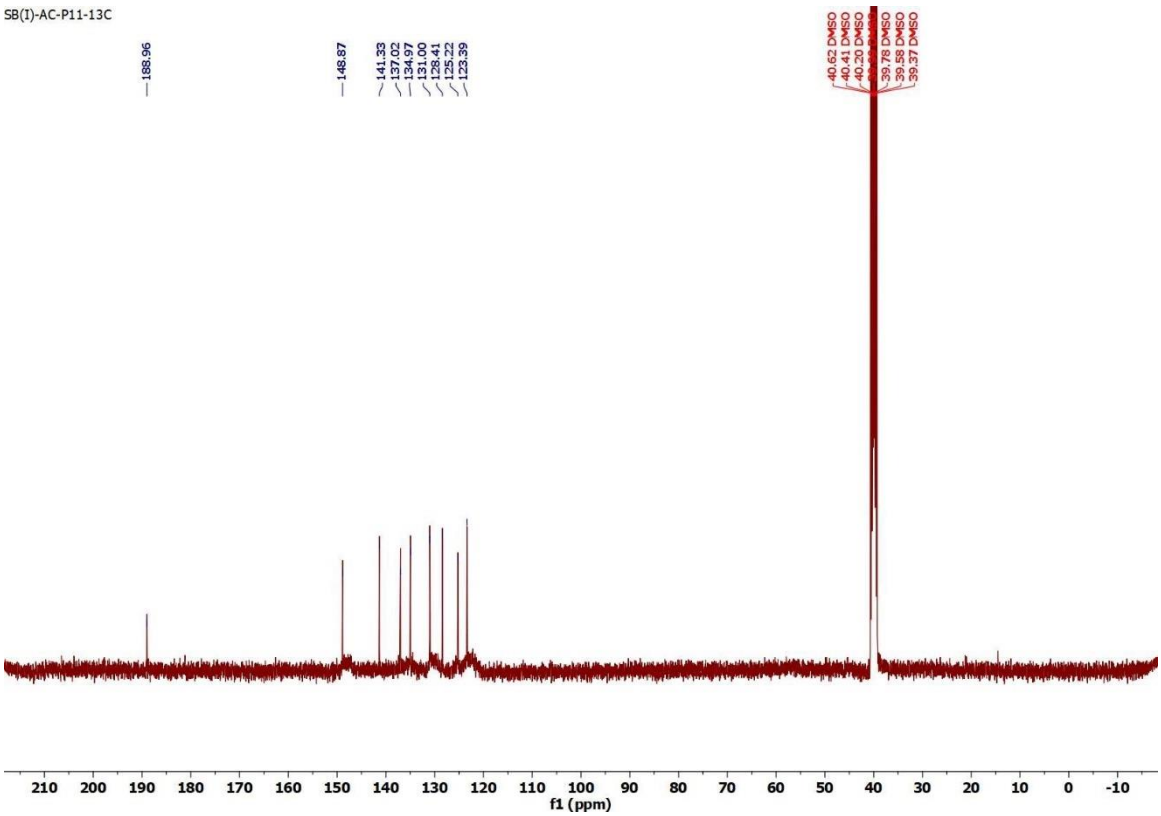

^{13}C NMR spectrum of **P$_{11}$** in DMSO-d$_6$

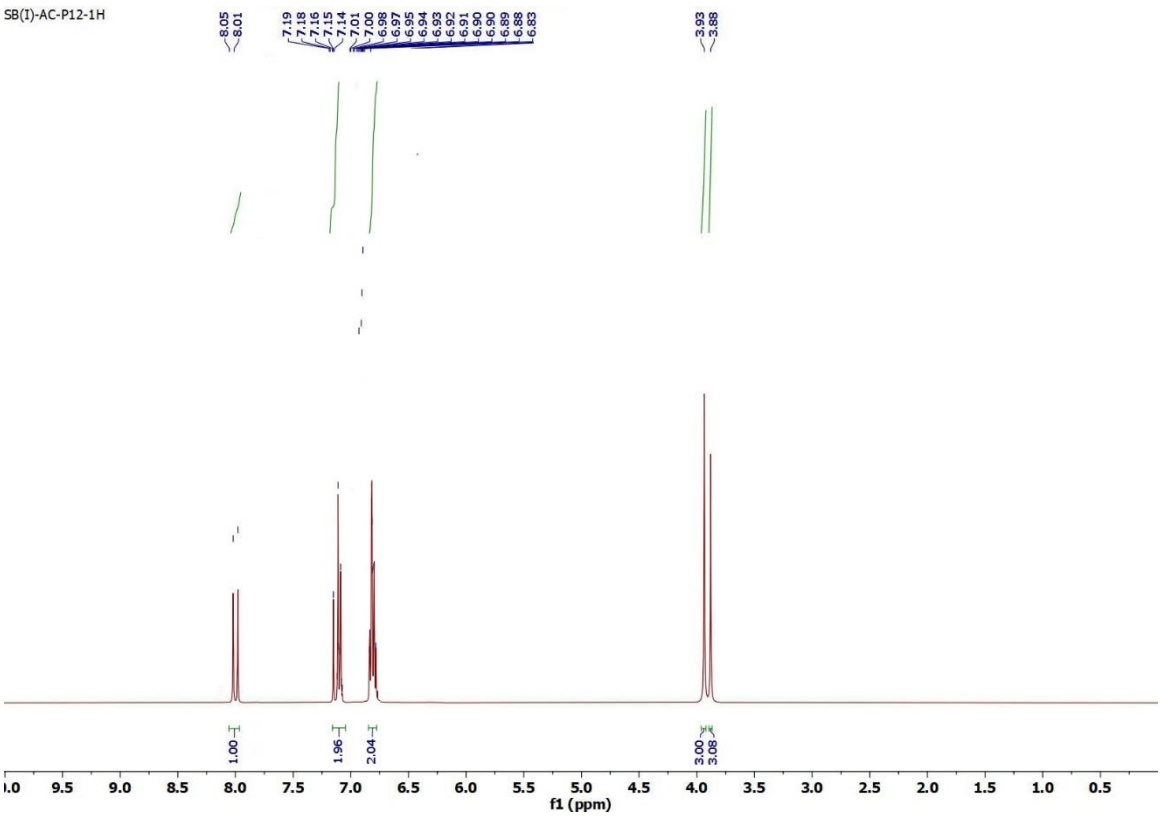

^{1}H NMR spectrum of **P12** in $CDCl_3$

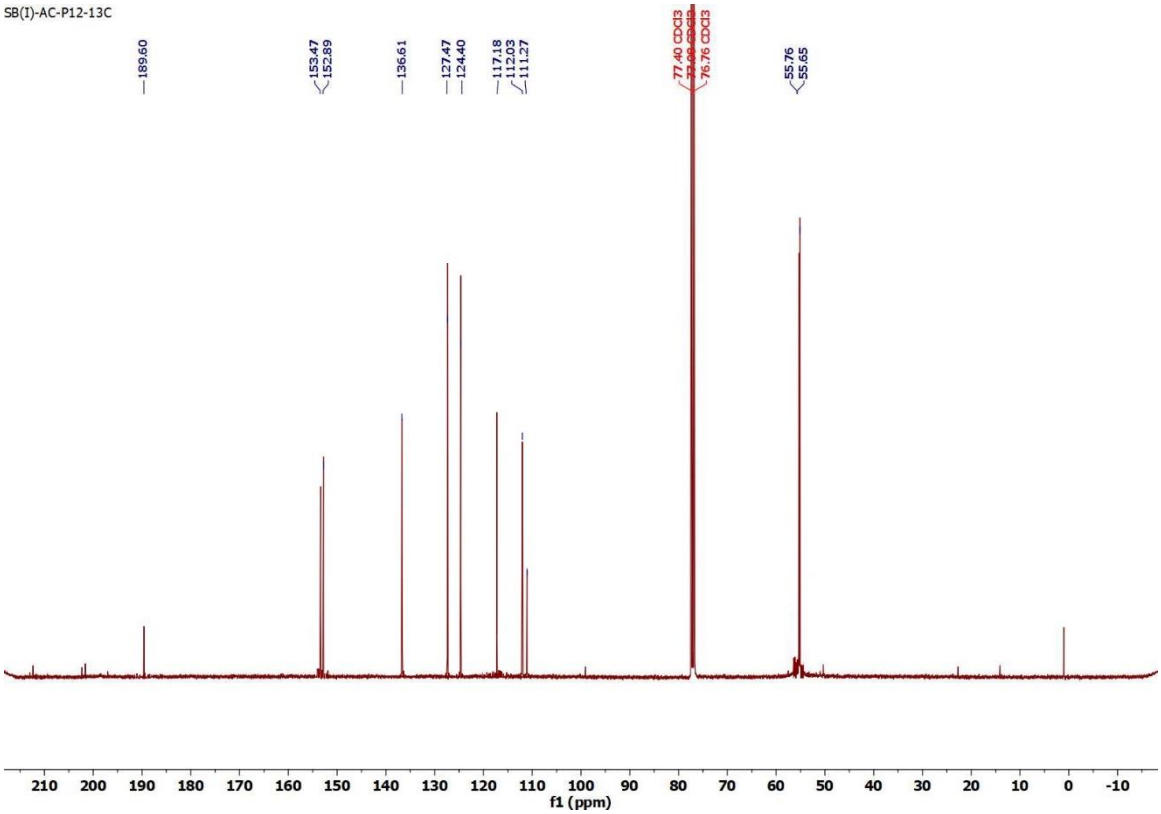

^{13}C NMR spectrum of **P12** in $CDCl_3$

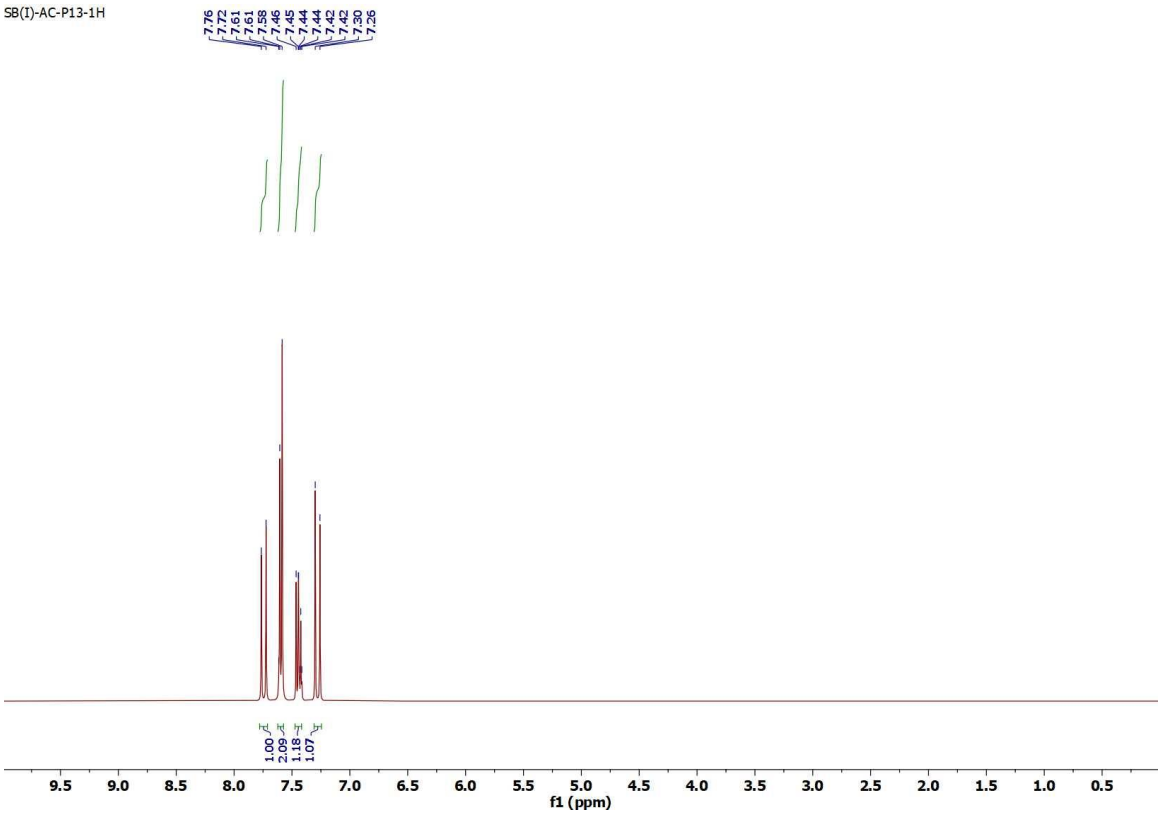

^{1}H NMR spectrum of **P$_{13}$** in DMSO-d$_6$

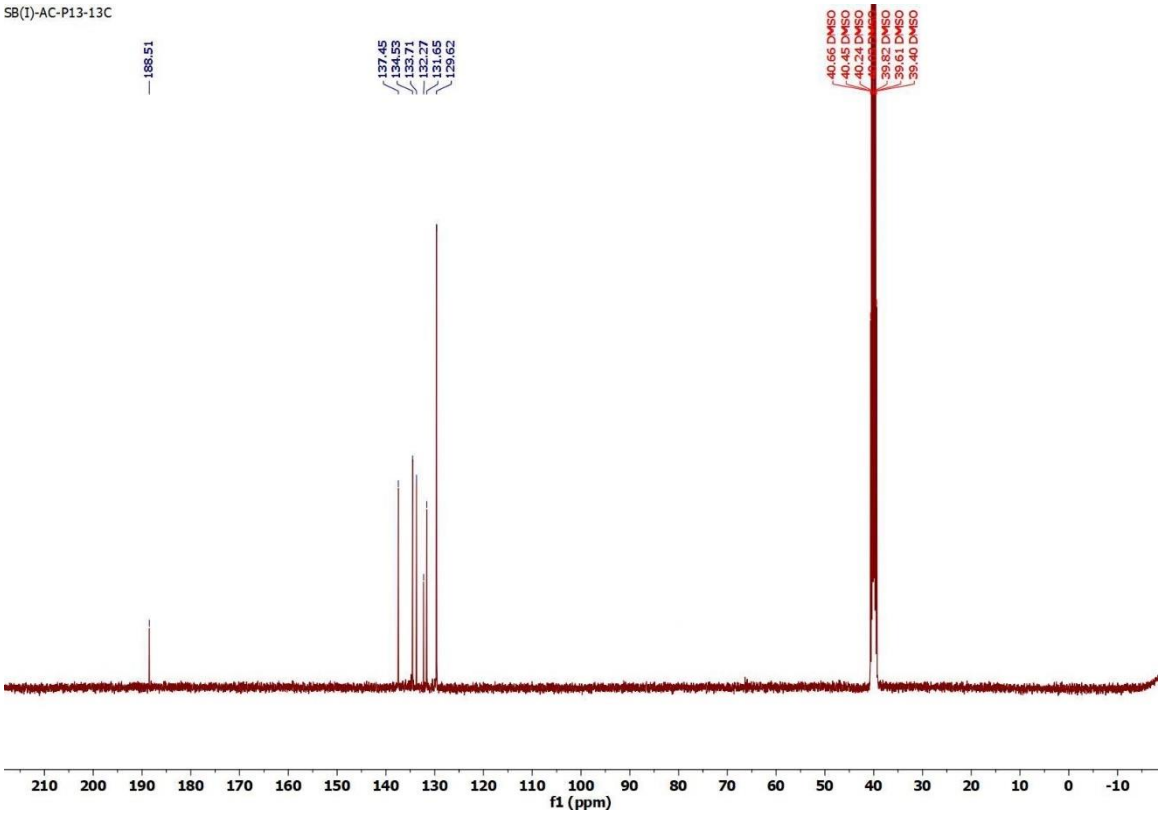

^{13}C NMR spectrum of **P$_{13}$** in DMSO-d$_6$

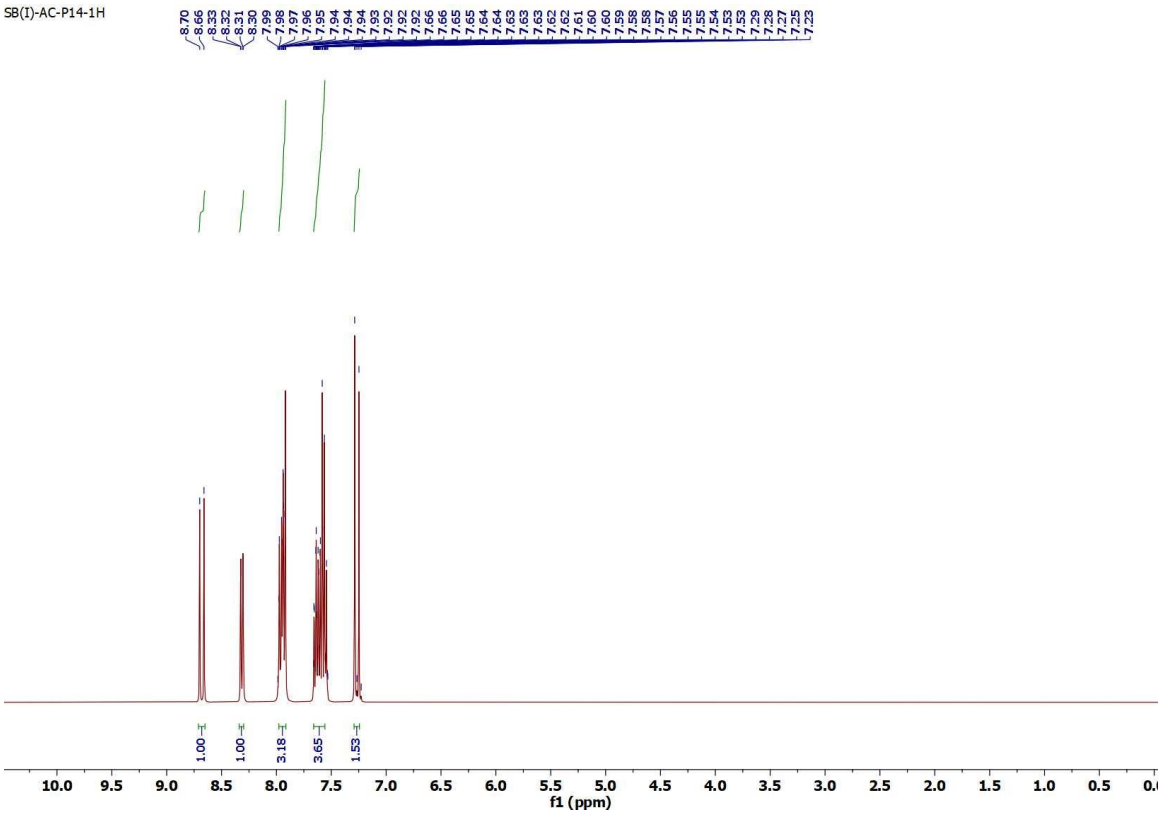

^{1}H NMR spectrum of **P$_{14}$** in $CDCl_3$

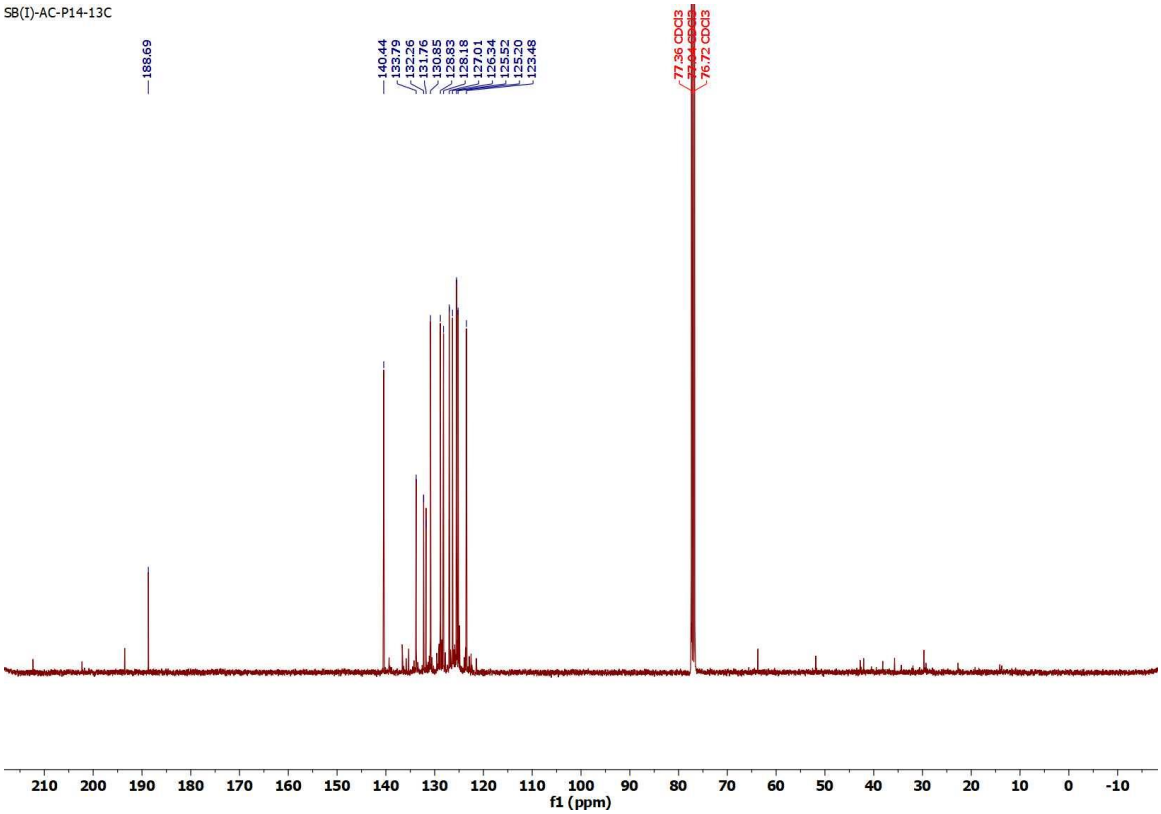

^{13}C NMR spectrum of **P$_{14}$** in $CDCl_3$

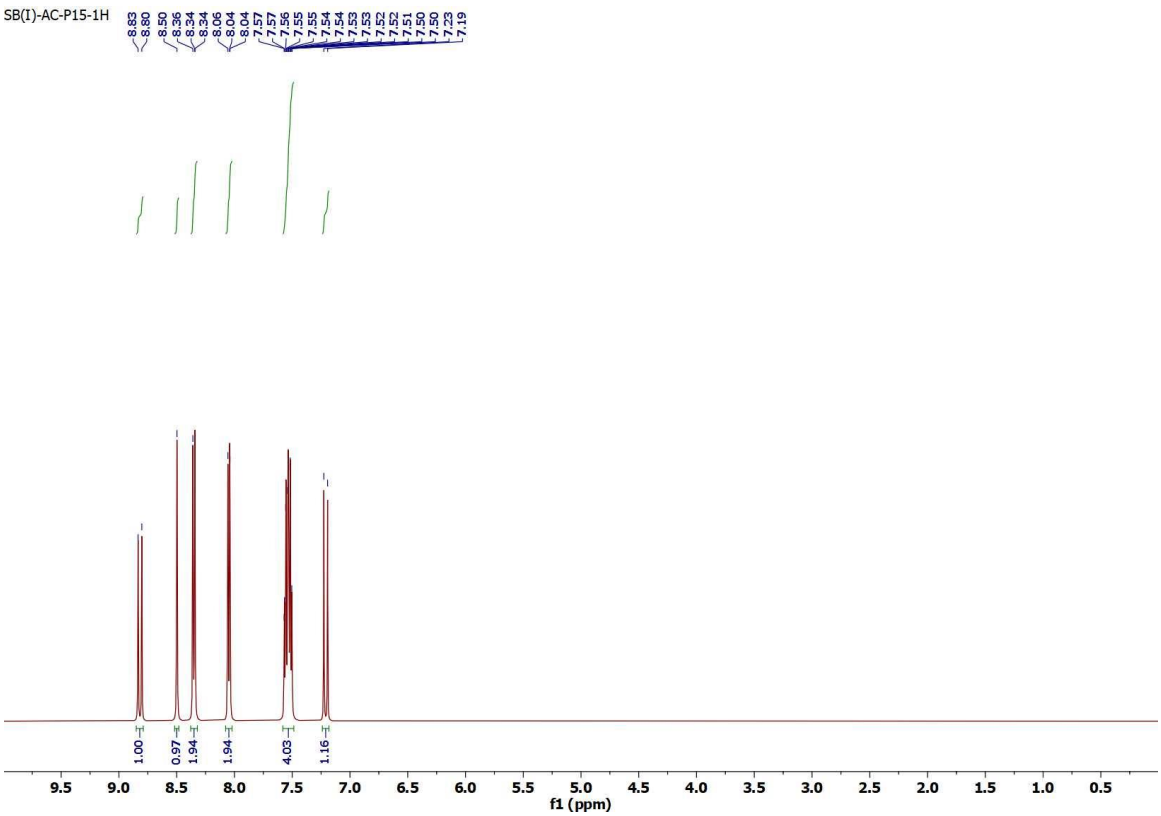

^{1}H NMR spectrum of **P$_{15}$** in $CDCl_3$

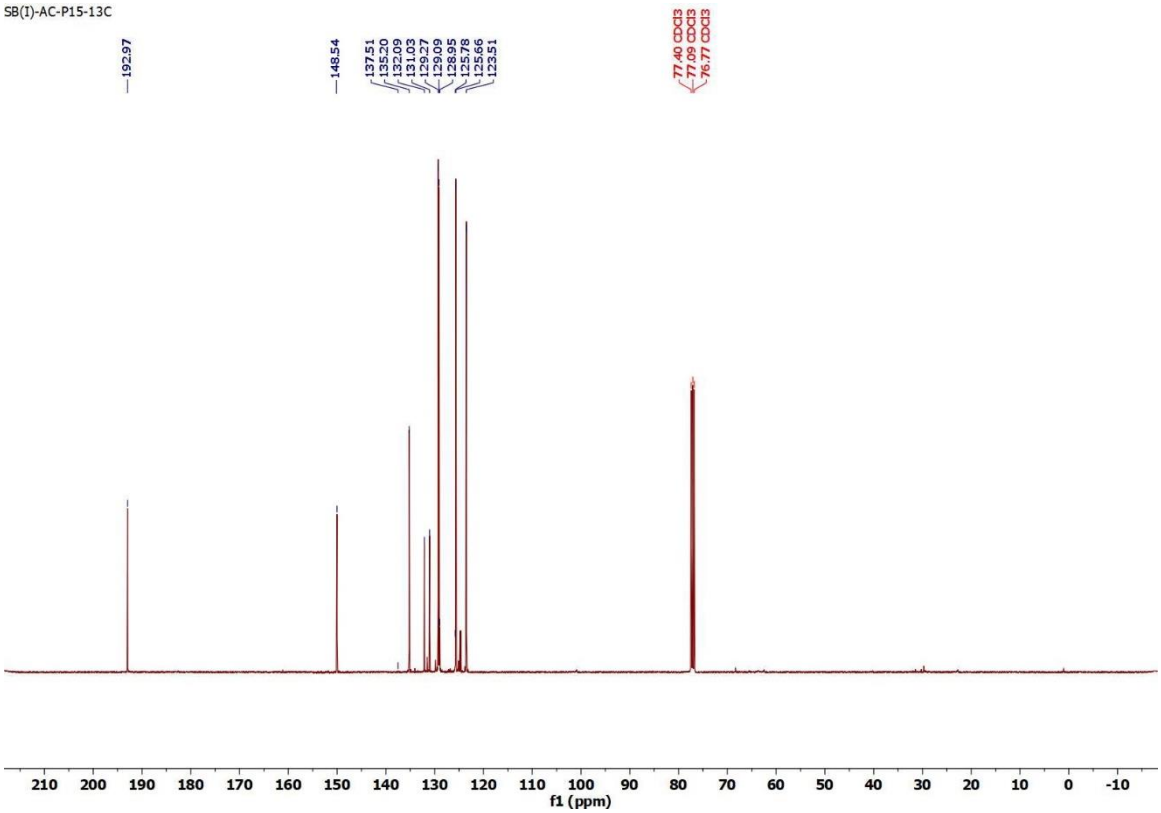

^{13}C NMR spectrum of **P$_{15}$** in $CDCl_3$

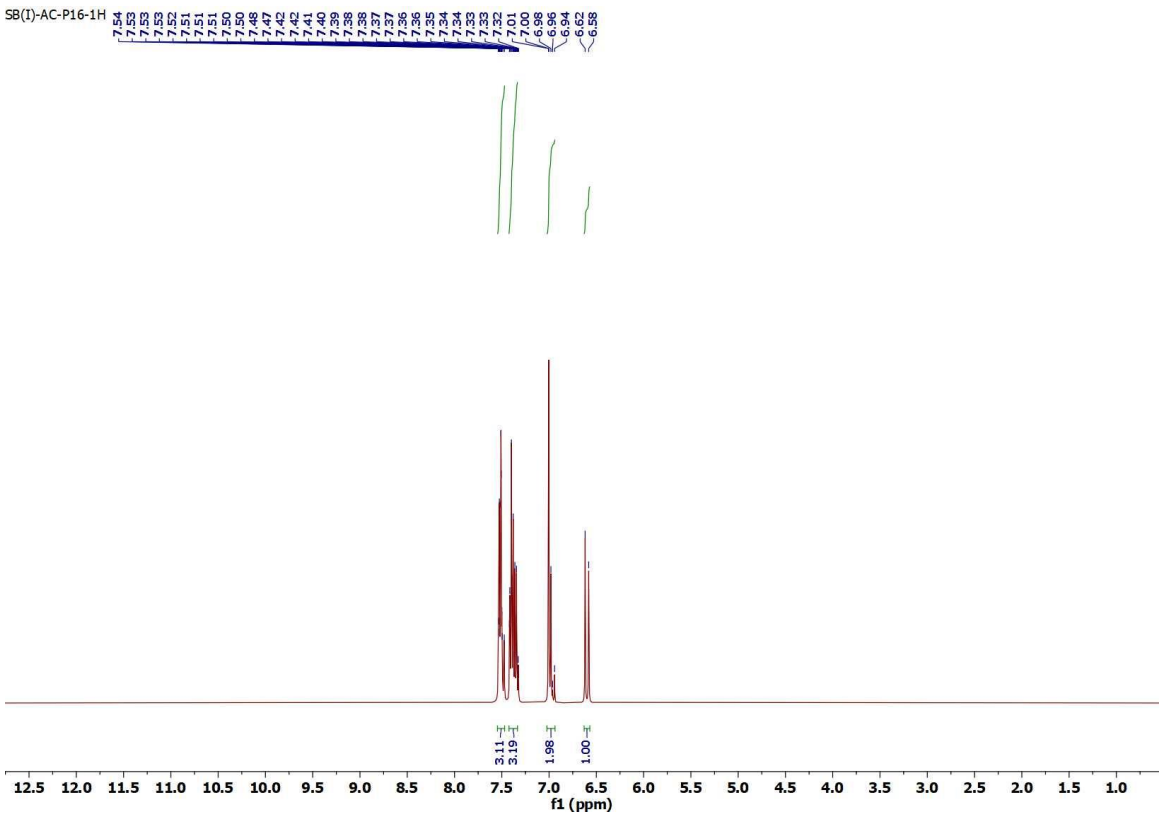

^{1}H NMR spectrum of **P_{16}** in $CDCl_3$

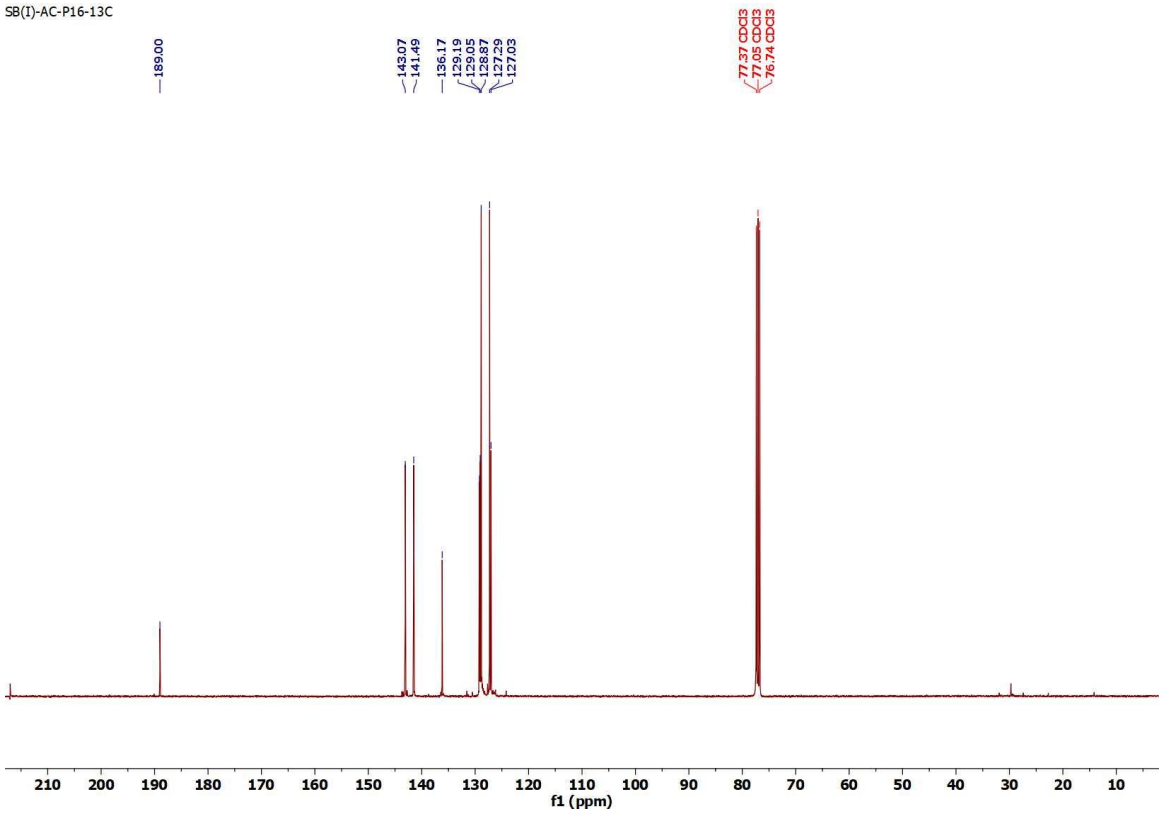

^{13}C NMR spectrum of **P_{16}** in $CDCl_3$

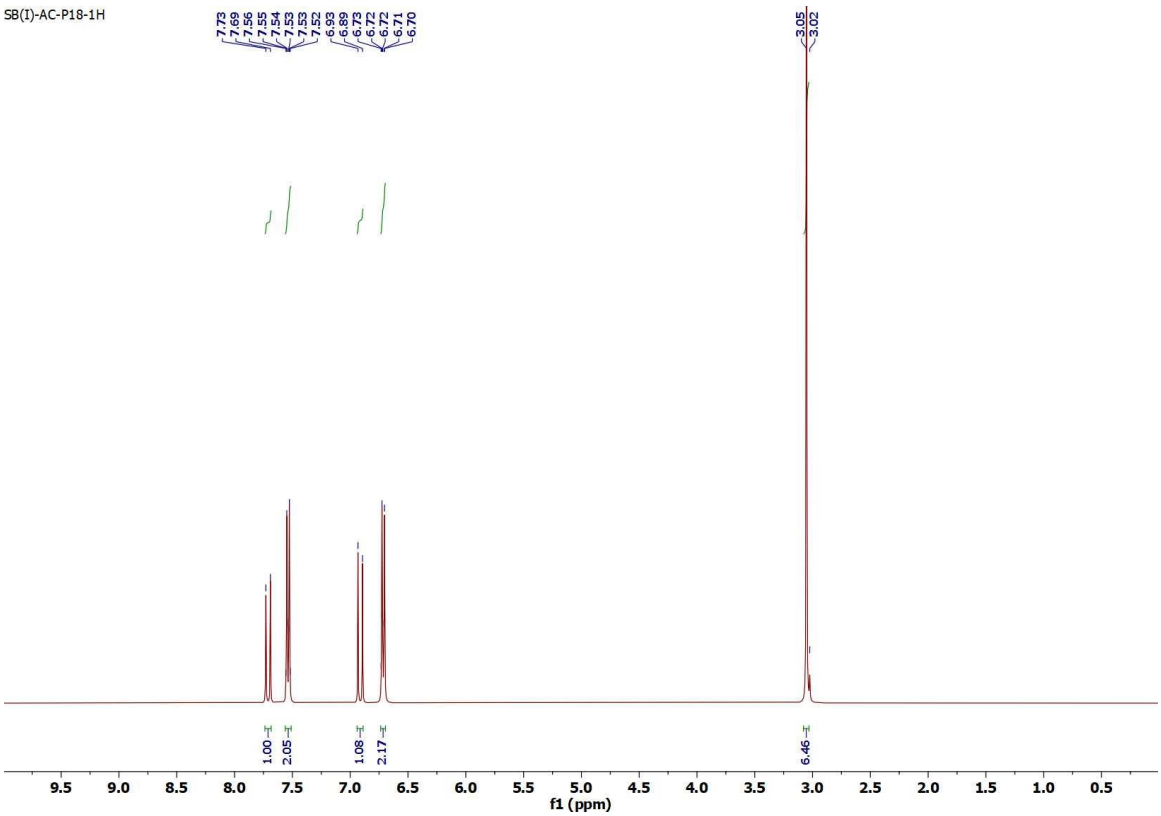

^{1}H NMR spectrum of **P$_{18}$** in $CDCl_3$

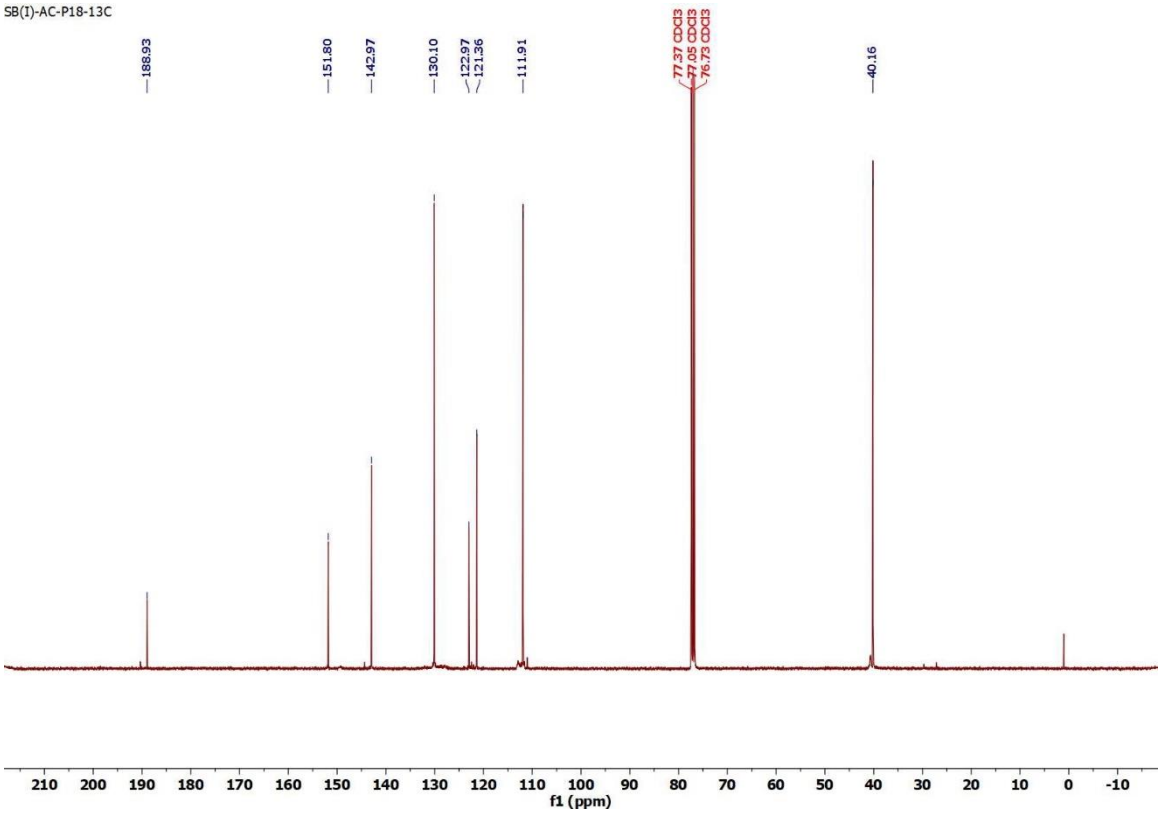

^{13}C NMR spectrum of **P$_{18}$** in $CDCl_3$

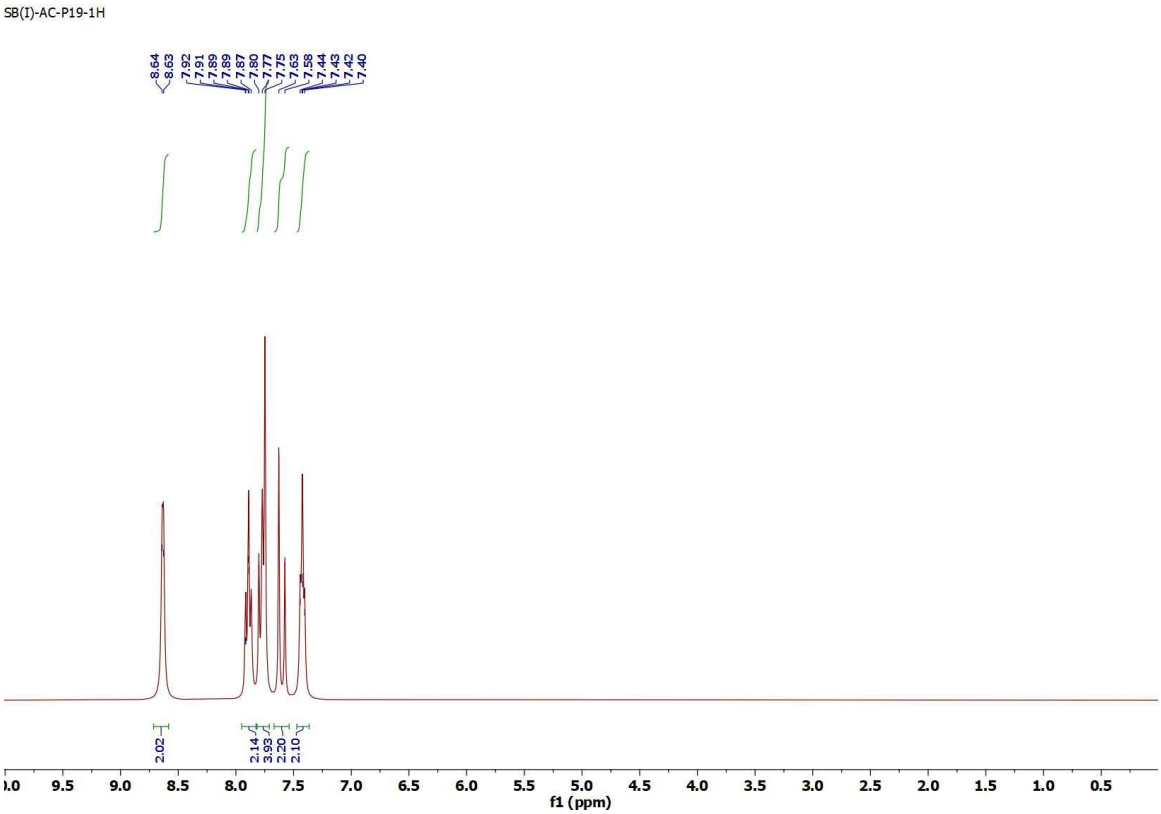

^{1}H NMR spectrum of **P_{19}** in CD_3OD

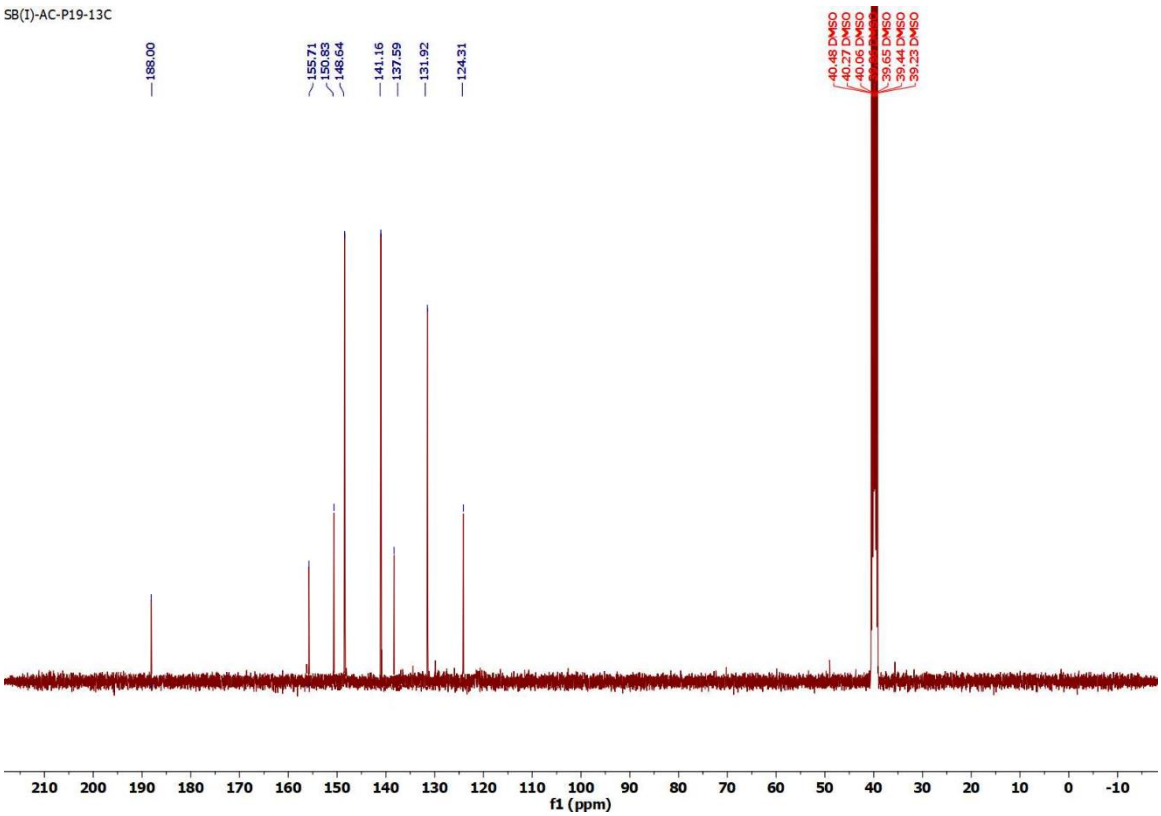

^{13}C NMR spectrum of **P_{19}** in DMSO-d_6

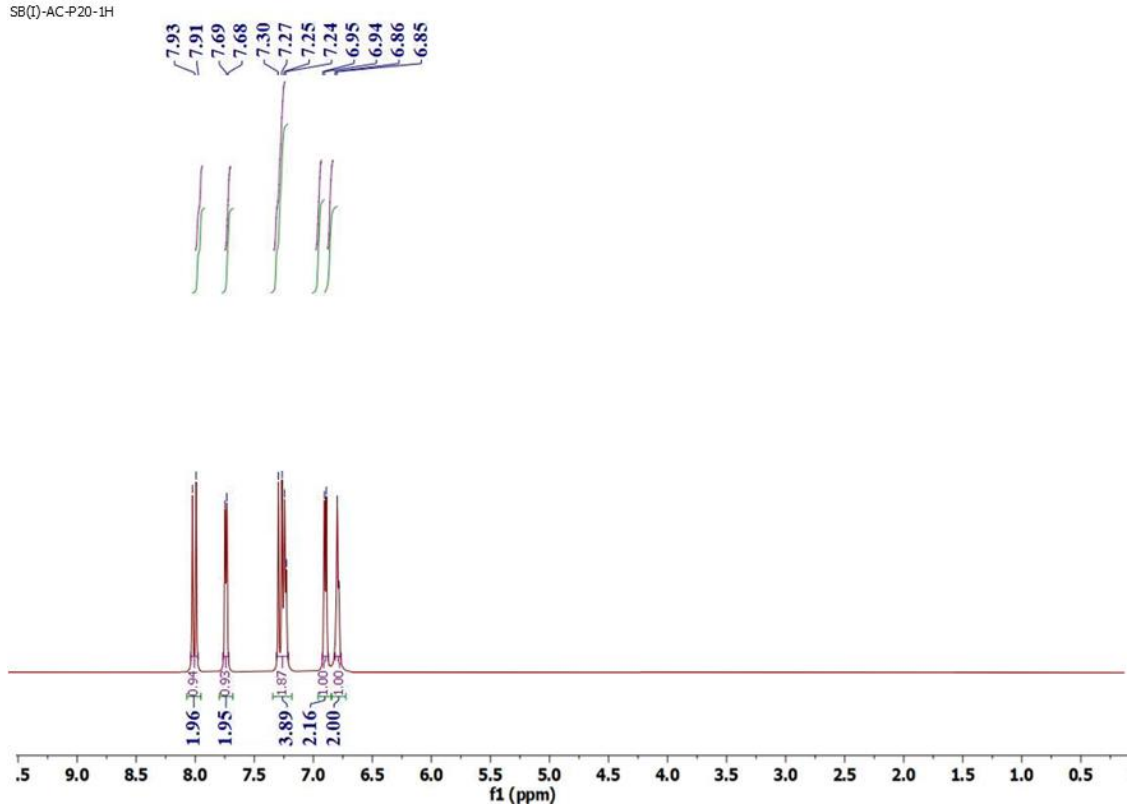

^{1}H NMR spectrum of **P20** in $CDCl_3$

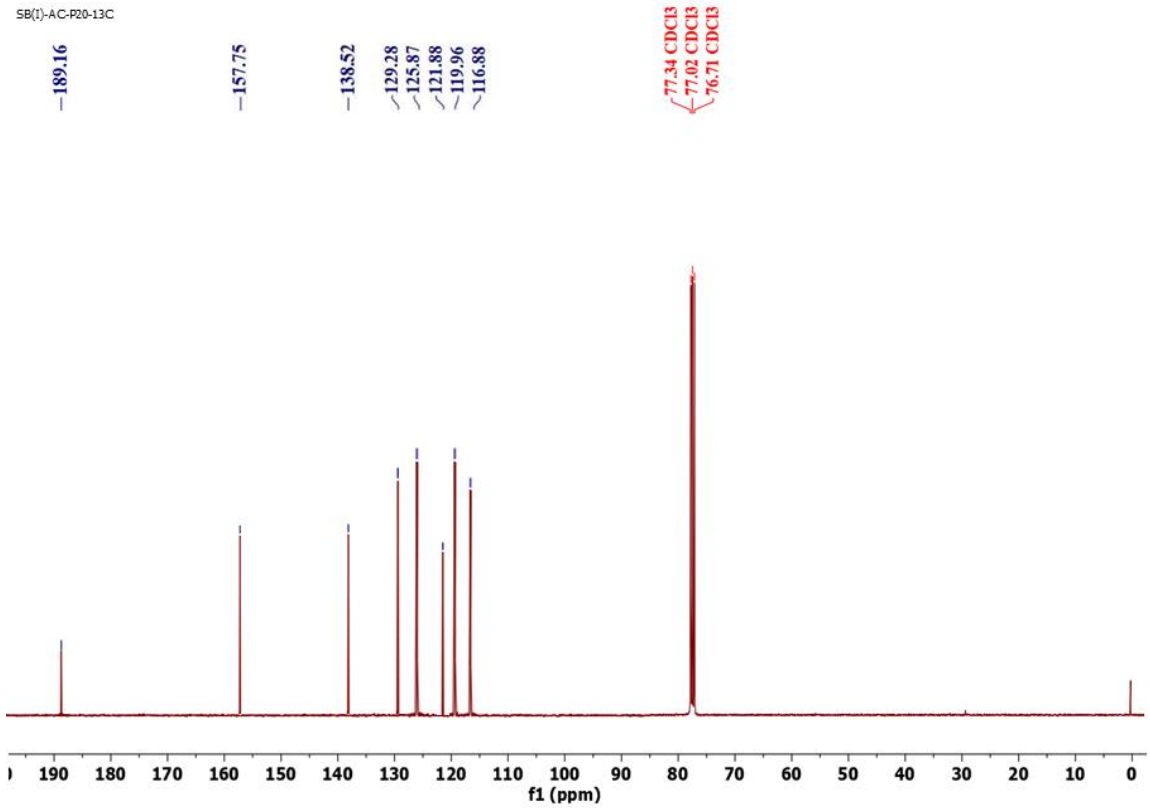

^{13}C NMR spectrum of **P20** in $CDCl_3$

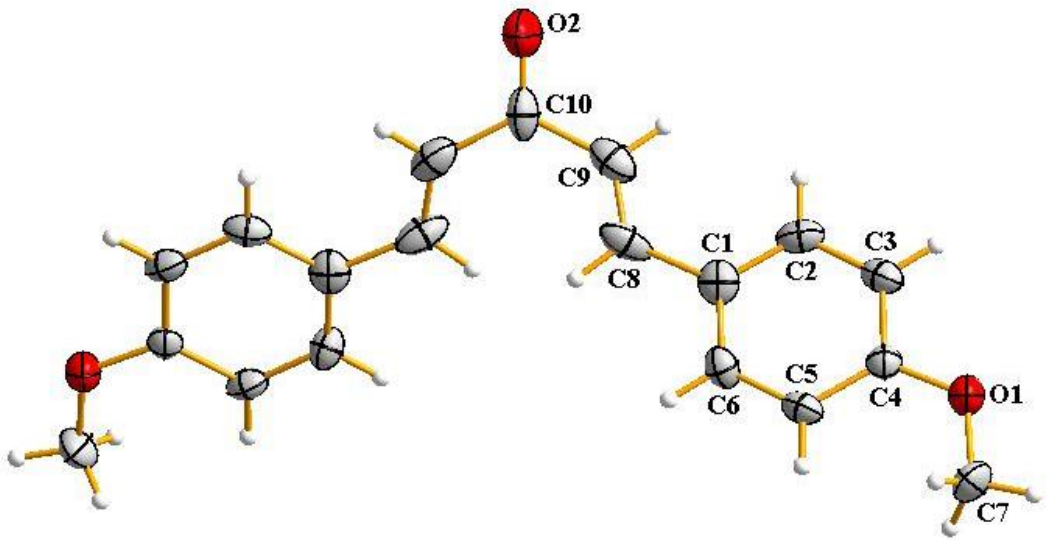

Fig. S17 Molecular structure of 1,5-bis-(4-methoxyphenyl)-penta-1,4-(*E*,*E*)-dien-3-one (**P2**).

Table S20 Selected bond distances and bond angles for **P2**

Bond distances (Å)			
C1-C8	1.520(9)	C10-O2	1.199(13)
C8-C9	1.272(10)	C4-O1	1.352(6)
C9-C10	1.497(10)	C7-O1	1.432(9)
Bond angles (°)			
C1-C8-C9	124.3(6)	C9-C10-C9	126.0(12)
C8-C9-C10	125.7(8)		

Table S21 Comparison of different catalysts for the crossed-aldol reactions

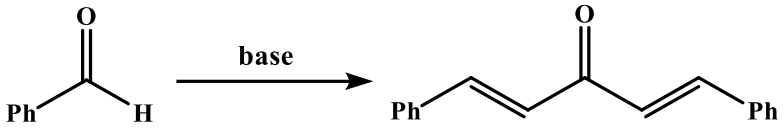

Entry	Base loading	Condition	TON	TOF (h^{-1})	Reference
1	1 mmol	75 ˚C, 15 h	1.6	0.11	**27a**
2	2 mol%	MW (1250 W), 3 min	49.5	990*	**27b**
3	20 mol%	90 ˚C, 45 h	2.75	0.06	**27c**
4	0.5 mol%	83 ˚C, 6 h	160	26.67	**This work**

* This data is for a catalytic reaction carried out using micro-wave.

Table S22 Crystallographic data for $[Ru(L^1)_2(dmso)_2]$ and $[Ru(L^2)_2(dmso)_2]$

Sample	$[Ru(L^1)_2(dmso)_2]$	$[Ru(L^2)_2(dmso)_2]$
empirical formula	$C_8H_{18}O_4S_6Ru$	$C_{10}H_{22}O_4S_6Ru$
Fw	471.61	499.77
Space group	Orthorhombic, Ibca	Orthorhombic, Pbca
a (Å)	10.3358(10)	11.6867(16)
b (Å)	11.1063(10)	11.6375(16)
c (Å)	30.191(3)	29.571(4)
α (◦)	90	90
β (◦)	90	90
γ (◦)	90	90
V (Å^3)	3465.7(6)	4021.8(10)
Z	8	8
Crystal size (mm)	0.16 × 0.18 × 0.18	0.10 × 0.18 × 0.20
T (K)	273	273
μ (mm^{-1})	1.628	1.410
R1[a]	0.0380	0.0385
wR2[b]	0.1466	0.1444
GOF[c]	1.23	1.15

[a] $R1 = \Sigma ||F_o| - |F_c|| / \Sigma |F_o|$.

[b] $wR2 = [\Sigma\{w(F_o^2-F_c^2)^2\}/\Sigma\{w(F_o^2)\}]^{1/2}$.

[c] $GOF = [\Sigma(w(F_o^2-F_c^2)^2)/(M-N)]^{1/2}$, where M is the number of reflections and N is the number of parameters refined.

Table S23 Crystallographic data for $[Ru(L^3)_2(dmso)_2]$ and $[Ru(L^4)_2(dmso)_2]$

Sample	$[Ru(L^3)_2(dmso)_2]$	$[Ru(L^4)_2(dmso)_2]$
empirical formula	$C_{12}H_{26}O_4S_6Ru$	$C_{14}H_{30}O_4RuS_6$
Fw	527.82	555.98
Space group	Monoclinic, C2/c	Orthorhombic, Ibca
a (Å)	13.9281(11)	10.3525(7)
b (Å)	16.4456(13)	11.1613(8)
c (Å)	9.3353(8)	30.316(2)
α (◦)	90	90
β (◦)	94.318(2)	90
γ (◦)	90	90
V ($Å^3$)	2132.2(3)	3502.93(40)
Z	4	8
Crystal size (mm)	0.16 × 0.22 × 0.24	0.14 × 0.18 × 0.22
T (K)	273	273
μ (mm^{-1})	1.335	1.618
R1[a]	0.0186	0.0404
wR2[b]	0.1134	0.0810
GOF[c]	1.05	1.080

[a] $R1 = \Sigma \, ||F_o| - |F_c|| / \Sigma |F_o|$.

[b] $wR2 = [\Sigma\{w(F_o^2-F_c^2)^2\}/\Sigma\{w(F_o^2)\}]^{1/2}$.

[c] $GOF = [\Sigma(w(F_o^2-F_c^2)^2)/(M-N)]^{1/2}$, where M is the number of reflections and N is the number of parameters refined.

Table S24 Crystallographic data for $[Ru(L^3)_2(bpy)]$ and 1,5-Bis-(4-methoxyphenyl)-penta-1,4-(*E*,*E*)-dien-3-one (**P_2**)

Sample	$[Ru(L^3)_2(bpy)]$	**P_2**
empirical formula	$C_{18}H_{22}N_2O_2RuS_4$	$C_{19}H_{18}O_3$
Fw	527.70	294.33
Space group	Monoclinic, $P2_1/n$	Orthorhombic, Aba2
a (Å)	12.6625(4)	7.4066(5)
b (Å)	11.4820(4)	34.011(2)
c (Å)	16.5225(6)	6.1761(4)
α (◦)	90	90
β (◦)	105.7030(10)	90
γ (◦)	90	90
V ($Å^3$)	2312.56(14)	1555.8 (17)
Z	4	4
crystal size (mm)	0.18 × 0.22 × 0.24	0.05 × 0.14 × 0.24
T (K)	273	273
μ (mm^{-1})	1.061	0.081
R1[a]	0.0281	0.1111
wR2[b]	0.1203	0.2520
GOF[c]	0.975	1.445

[a] $R1 = \Sigma ||F_o| - |F_c|| / \Sigma |F_o|$.

[b] $wR2 = [\Sigma\{w(F_o^2-F_c^2)^2\}/\Sigma\{w(F_o^2)\}]^{1/2}$.

[c] $GOF = [\Sigma(w(F_o^2-F_c^2)^2)/(M-N)]^{1/2}$, where M is the number of reflections and N is the number of parameters refined.